

1 **Evaluating the Sustainability of Groundwater Resources: A**
2 **Framework Incorporating the Ecological Groundwater Depth and**
3 **Reliability, Resilience, and Vulnerability Indexes**

4

5 Mingjun Wang¹, Bo Xu^{1*}, Chi Zhang^{1*}, Yong Peng¹, Yu Li¹, Bing Yu¹, Xinqiang Du²

6 ¹School of Infrastructure Engineering, Dalian University of Technology, Dalian, China

7 ²College of New Energy and Environment, Jilin University, Changchun, China

8

9 **Corresponding Author:** Bo Xu (xubo_water@dlut.edu.cn), Chi Zhang (czhang@dlut.edu.cn)

10

11 **Key Points:**

- 12 • A framework is proposed to evaluate the sustainability of groundwater resources under the
13 impacts of climate change and/or human activities.
- 14 • The framework considers multiple targets to calculate the ecological groundwater depth with
15 spatial heterogeneity and temporal dynamics.
- 16 • The framework incorporates reliability, resilience, and vulnerability to evaluate the
17 sustainable performance of groundwater resources.

18

Abstract

Groundwater resource sustainability faces significant challenges due to groundwater overdraft and waterlogging. Here we propose a novel framework for evaluating the sustainability of groundwater resources. The framework incorporates a dynamic calculation of the ecological groundwater depth (EGWD) at the grid scale, considering multiple protective targets. To quantitatively evaluate the groundwater sustainability, we utilize reliability, resilience, and vulnerability, to measure the frequency, duration, and extent of unsatisfactory conditions. We apply this framework to the lower part of Tao'er River Basin in China. During the non-growth period and growth period, the upper thresholds of the EGWD range from 1.16 to 2.05 meters and 1.16 to 4.05 meters, respectively. The lower thresholds range from 6.28 to 33.54 meters and 4.87 to 30.72 meters, respectively. Future climate change improves reliability performances in regions with deep groundwater depths. Although the precipitation infiltration increases in future scenarios, prolonged duration and enhanced intensity of extreme climate events lead to decreased resilience and vulnerability performances under climate change. The proportion of areas with resilience values less than 1/12 expands to 2~3 times that of the historical scenario. Furthermore, we observe that more areas face the dual challenges of groundwater depletion and waterlogging under future climate change, particularly in high-emission scenarios. This study enhances understanding of groundwater resource sustainability by considering the spatial-temporal distribution of the EGWD, climate change impacts, and the identification of key regions for management. The insights can inform the development of effective strategies for sustainable groundwater resource management.

Key words: groundwater resource sustainability; ecological groundwater depth; reliability-resilience-vulnerability; climate change; groundwater resource management

1 Introduction

Groundwater, as the largest accessible freshwater resource, plays an increasingly prominent role in providing freshwater supply and accounts for approximately one-third of global freshwater extractions (Doll et al., 2012; Famiglietti, 2014; Gorelick & Zheng, 2015). Proper management of

groundwater resources is essential for ensuring long-term water supply for both human and ecosystem needs, particularly within the ambit of compounded climatic shifts and anthropogenic interventions (Mays, 2013). However, in regions with limited access to surface water, escalating demands often result in groundwater overdraft. Managing groundwater resources in such areas becomes challenging, as they must address a wide range of issues associated with global change, including damages on groundwater-dependent ecosystems, groundwater depletion, land subsidence, seawater intrusion, and deterioration of groundwater quality (Dangar et al., 2021; Duran-Llacer et al., 2022; Gejl et al., 2019; Kumar et al., 2022; Ye et al., 2016). Furthermore, regions characterized by shallow groundwater depths, caused by excessive irrigation and poor drainage, experience soil salinization and waterlogging (Metternicht and Zinck, 2003; Moreira et al., 2015; Singh, 2014; Wang et al., 2021). This phenomenon significantly affects the environment and agricultural safety in these areas. It is evident that the sustainable management of groundwater resources faces significant threats under the combined effects of future climate change and human activities (Malekinezhad & Banadkooki, 2018; Scanlon et al., 2023).

The concept of groundwater sustainability is initially proposed by Alley et al. (1999) and has since undergone continuous refinement and development. Groundwater sustainability is defined as the capacity of groundwater systems to consistently provide a consistent supply of sufficient and high-quality water for both ecosystems and human society (Ruan and Wu, 2022). Prior research has presented two approaches to evaluate groundwater sustainability. The first approach focuses on estimating groundwater storage using satellite remote sensing to calculate sustainability indexes, such as GRACE-groundwater drought index, for the evaluation of groundwater resource sustainability (Thomas, 2019; Thomas, Famiglietti, Landerer, et al., 2017; Thomas, Caineta & Nanteza, 2017). The second approach aims to establish a comprehensive evaluation framework that considers various aspects, including resources, economy, and ecology (Bui et al., 2018; Karimi et al., 2022; Samani et al., 2021). It evaluates the sustainability of groundwater resources and ascertain the degree of sustainability using various indexes such as groundwater sustainability infrastructure index (Pandey et al., 2011) and groundwater sustainability index (Singh & Bhakar, 2021). The above two kinds of evaluation approach are both based on the groundwater storage.

Groundwater depth, as the most tangible variable of groundwater resources, provides a more

direct insight into the interplay between underground aquifers and ecological contexts. Unlike groundwater storage, groundwater depth facilitates a quantitative correlation with factors such as soil salinization, vegetation growth, and land subsidence, thereby enabling efficient evaluation of groundwater resource sustainability (Yang et al., 2019; Zhang et al., 2022). Ecological groundwater depth (EGWD), comprising upper and lower thresholds (Zhang, 1981; Zhang et al., 2003), serves as a criterion to determine whether groundwater depths remain within an appropriate range. Various targets, such as soil salinization (Singh, 2014), vegetation degradation (Huang et al., 2019; Kath, 2018), land subsidence (Ye et al., 2016), and aquifer depletion (Konikow and Kendy, 2005), are employed to establish the EGWD.

However, previous studies have primarily focused on calculating the EGWD predicated upon individual protection target in a region thus neglecting the coupling impacts of multiple protection targets. Different areas have diverse protection targets, the requirements of which on groundwater depth also vary in different seasons. It may lead to incomplete consideration of the spatial heterogeneity and temporal dynamics of the EGWD. Furthermore, while various indicators and criteria have been proposed to evaluate groundwater sustainability based on groundwater storage and depths, these measures exhibit a gap in providing a comprehensive evaluation of groundwater resource sustainability that incorporates the frequency, duration, and extent of unsatisfactory states within the groundwater system.

To fill the above research gaps, this paper proposes a novel framework for evaluating the sustainability of groundwater resources. Initially, we calculate the dynamic EGWD at the grid scale, incorporating a multitude of protection targets as criteria to ascertain suitable ranges of groundwater depths. Subsequently, an integrated surface water and groundwater model incorporating diverse scenarios of interests to decision makers is developed to simulate variations of groundwater depths. Finally, we deploy a suit of evaluation indexes encompassing reliability, resilience, and vulnerability (RRV) to quantitatively measure the frequency, duration, and extent of groundwater depths surpassing threshold ranges of the EGWD. These indexes, entrenched within the domain of water supply operation of reservoirs (Cai et al., 2002; Hashimoto et al., 1982; McMahon et al., 2006; Sandoval-Solis et al., 2011; Zhang et al., 2017), offer a holistic evaluation of groundwater resource sustainability by drawing an analogy between fluctuations in

groundwater depth and the operational dynamics of reservoir systems. We apply this framework to the lower reach of the Tao'er River Basin (LTRB) in Northeast China. By evaluating the sustainability of groundwater resources under future climate change, the framework identifies key areas within the LTRB necessitating targeted groundwater resource stewardship, thus engendering consequential insights pertinent to the realm of sustainable management strategies.

The subsequent sections of this paper are structured as follows. Section 2 presents the detailed framework for evaluating groundwater resource sustainability, while Section 3 provides an overview of the LTRB's fundamental characteristics and the application of the evaluation framework within the basin. Section 4 discusses the spatial-temporal distribution of the EGWD, the RRV performances of the groundwater system under climate change, groundwater resource sustainability issues, and the identification of key areas for future management. Finally, Section 5 encapsulates the synthesis of findings generated by this inquiry, the concomitant implications, the inherent limitations of this study, and prospective avenues for future work.

2 The Framework for Evaluating the Sustainability of Groundwater Resource

2.1 Overview

This study presents a novel conceptual framework for evaluating the sustainability of groundwater resources, consisting of three essential components (Figure 1): (1) the calculation of the EGWD, (2) the development of an integrated hydrological model incorporating diverse scenarios, and (3) the calculation of RRV indexes. The EGWD is regarded as the criterion to judge whether the groundwater depth remains in a reasonable range. The integrated hydrological model can accurately simulate long-term trajectories of groundwater depths in scenarios of interest to decision makers. For quantitatively evaluating the groundwater sustainability, the EGWD and simulation results of groundwater depths are used to calculate RRV indexes measuring the frequency, duration, and extent of unsatisfactory conditions. For a more intricate understanding of each component within the framework, please refer to sections 2.2~2.4 below.

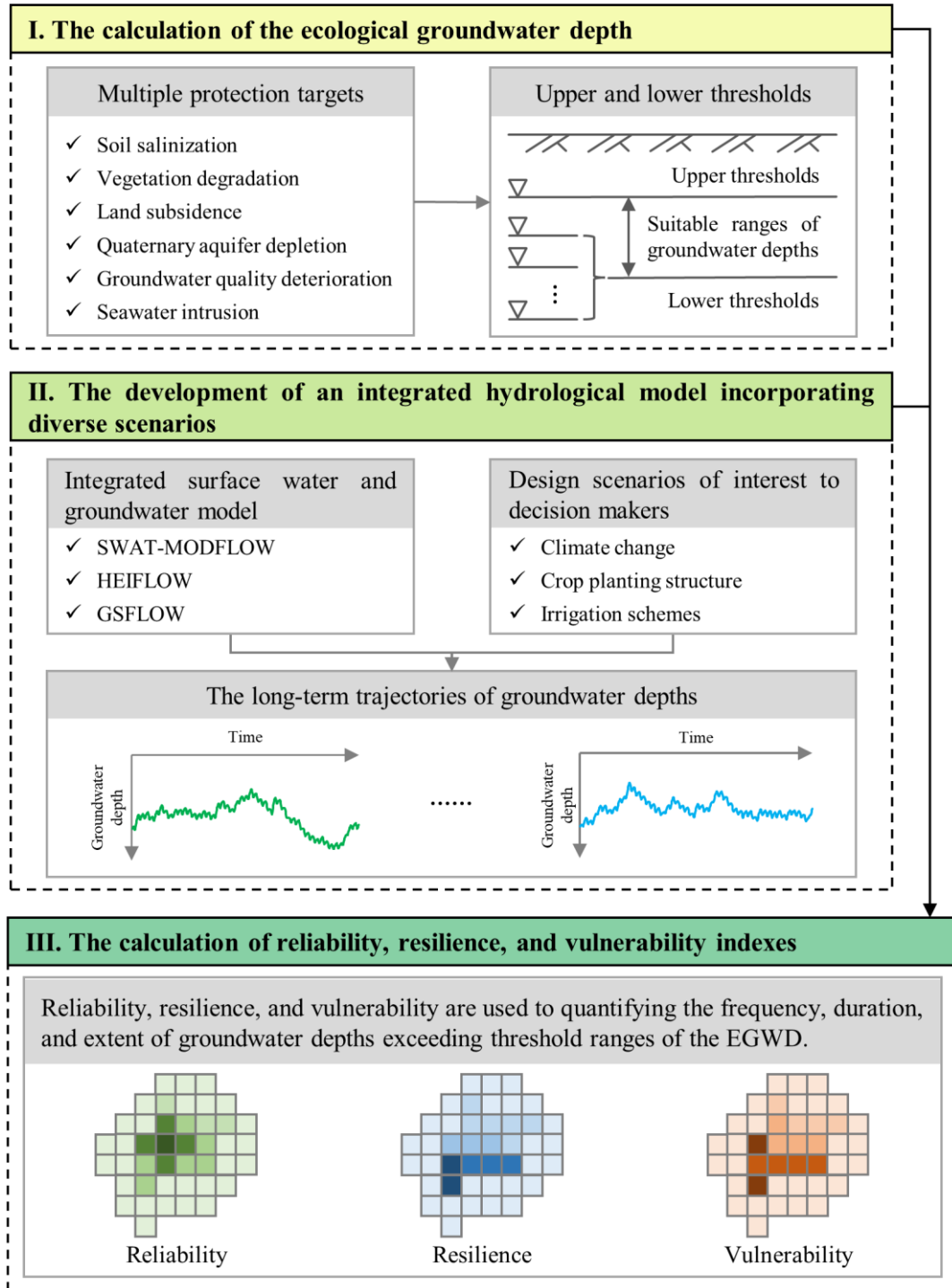


Figure 1 The framework for groundwater resource sustainability evaluation

2.2 Ecological Groundwater Depth

The EGWD refers to the groundwater depth that can satisfies the requirements of eco-environment without causing any deterioration, encompassing both upper and lower thresholds (Zhang, 1981; Zhang et al., 2003). In general, shallow groundwater depths may result in soil

salinization due to the strong soil evaporation with the moisture evaporating to the air and salts accumulating in the soil (Singh, 2021). Conversely, deep groundwater depths can give rise to various eco-geological environmental issues, such as vegetation degradation (Xu & Su, 2019), land subsidence (Ye et al., 2016), groundwater depletion (Konikow & Kendy, 2005), groundwater quality deterioration (Gejl et al., 2019), seawater intrusion (Tomaszkiewicz et al., 2014). The EGWD influenced by multiple protection targets (Figure 2), is dominated by different protection targets in distinct areas and time periods. To comprehensively evaluate the EGWD, this study synergistically integrates multiple protection targets, culminating in the computation of grid-scale EGWD across different temporal periods.

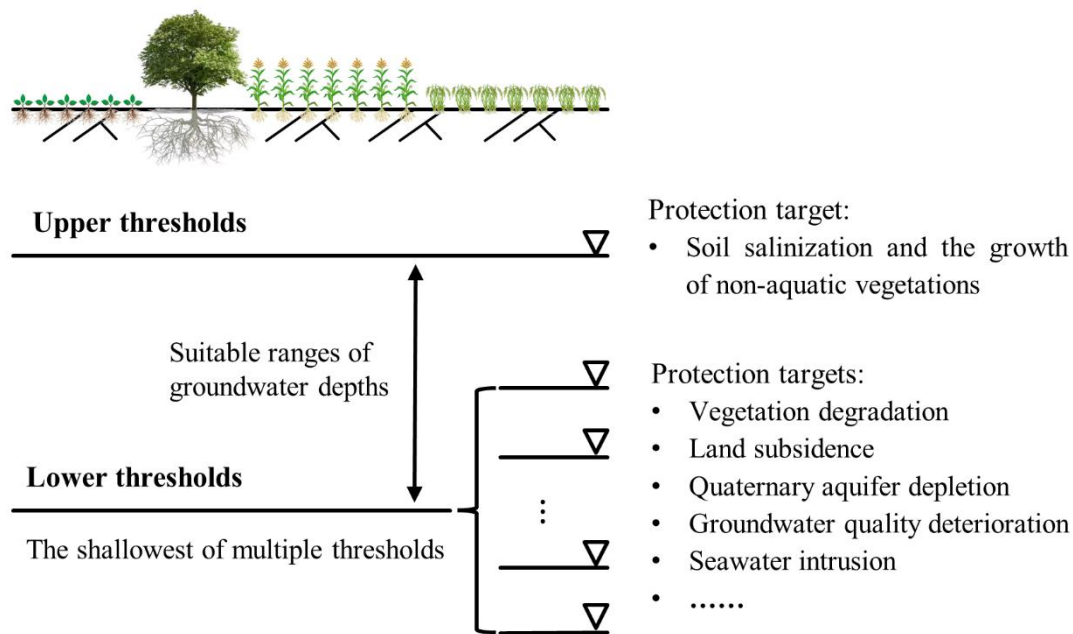


Figure 2 Schematic diagram of the ecological groundwater depth

2.2.1 Upper Thresholds of the Ecological Groundwater Depth

The upper threshold of the EGWD is primarily oriented towards the mitigation of soil salinization and the facilitation of optimal growth of non-aquatic vegetation species (Jia et al., 2015; Zhai et al., 2021). During the non-growth period spanning from November to April of the subsequent calendar year, vegetations undergoes phases of desiccation, senescence, mortality, or dormancy, leading to a diminished requirement for vegetation growth proliferation. During this phase, the groundwater depth necessary to prevent soil salinization is determined by the capillary

rise height. Conversely, encompassing the growth period spanning from May to October, the imperative groundwater depth for preempting soil salinization phenomena becomes a function of the summation between the capillary rise height and the depth of vegetation root systems. When the groundwater depth falls below the capillary rise height, groundwater recharges the soil through the capillarity, leading to high soil moisture and strong soil evaporation. The moisture transpiration process results in aqueous volatilization into the atmosphere, with concomitant accumulation of salts within the soil matrix, thereby instigating plausible events of soil salinization occurrences. Additionally, instances of shallow groundwater depths can exert an elevating influence upon soil moisture content and concurrently impose limitations upon effective soil aeration within the root zone. It thus becomes incumbent that the capillary rise height remains situated below the substratum spanned by the vegetation root depth during the growth period. In hydrological contexts dominated by perennial or seasonal surface water bodies, typified by aquatic ecosystems, the risk of soil salinization is minimal. Therefore, the upper threshold of the EGWD is not concerned within such aquatic settings (Lu, 2020).

The determination of the upper threshold of the EGWD involves two crucial parameters: the capillary rise height and the depth of vegetation root systems. The capillary rise height is subject to the physicochemical properties of the soil, and can be attained through scrutiny of controlled laboratory experimentation (Dong et al., 2008), the field investigation (Pan et al., 2018), and the computational application of empirical formulations (Useviciute & Baltreinaite-Gedienė, 2022). The vegetation root depth exhibits variations across disparate ecological settings, an outcome of the diversity in vegetation species and the differences of root systems spanning ecosystems encompassing paddy fields, drylands, grasslands, and woodlands. The maximum root depth of different vegetation species within a specific ecosystem is selected as the vegetation root depth for that ecosystem. For each vegetation species, the depth at which roots account for more than 80% of the total root length is considered as the root depth of that particular vegetation. Information on vegetation species and their respective root depths in various ecosystems can be obtained through field investigations or by referring to relevant literature and books (Lu, 2020; Zhao, 2012).

2.2.2 Lower Thresholds of the Ecological Groundwater Depth

The lower threshold of the EGWD is subject to the influence of multiple protection targets (Figure 2). Prolonged and intense groundwater exploitation can lead to a decline in regional groundwater level, thereby resulting in insufficient water supply to vegetation roots and consequent degradation of vegetation integrity (Meng et al., 2019; Zhang et al., 2011). This decline in groundwater level also transfers the load originally carried by groundwater to the soil particles, which increases the risk of land subsidence (Ye et al., 2016). Additionally, high-intensity groundwater exploitation may lead to the aquifer dewatering and groundwater depletion (Bierkens & Wada, 2019), significantly impairing groundwater resource sustainability. Apart from these overarching protection targets, specific areas may have unique protection needs. For example, in groundwater wellfield protection zones, the decline of the groundwater level facilitates the infiltration of the water with poor quality into the aquifer, leading to the groundwater quality deterioration (Yoneda et al., 2001). In coastal areas, low groundwater level easily causes seawater intrusion, resulting in saline groundwater (Tomaszkiewicz et al., 2014). Therefore, the calculation of the lower threshold of the EGWD necessitates a comprehensive analysis of specific protection requirements in different areas and time periods, considering appropriate protection targets.

(1) Groundwater depth thresholds for preventing vegetation degradation

Vegetation undergoes processes such as desiccation, senescence, mortality, or dormancy during the non-growth period, thereby making the target of preventing vegetation degradation insignificant. In agricultural areas, the groundwater depth threshold for mitigating vegetation degradation is ignored due to implementation of irrigation practices during periods of water deficiency. However, in grasslands, woodlands, and wetlands, this threshold is taken into account.

Previous studies have proposed two ideas for determining the groundwater depth threshold for preventing vegetation degradation. The first posits that groundwater will no longer support the vegetation growth when the groundwater depth exceeds the extreme evaporation depth. Hence, the extreme evaporation depth is regarded as the threshold (H_1) for preventing vegetation degradation (Fan et al., 2004; Pan et al., 2018). The extreme evaporation depth relies on soil properties and can be obtained through numerical simulations (Shah et al., 2007), lysimeter measurements (Ma et al., 2019), empirical formula calculations (Fu et al., 2008), and dynamic data correlation methods

(Zhao, 2012).

The second idea involves analyzing the relationship between the actual growth state of vegetation and groundwater depth to determine the threshold (H_2) for preventing vegetation degradation (Huang et al., 2019; Jia et al., 2015; Kath, 2018). To encapsulate the growth status of vegetation accurately, precise vegetation indexes are embraced, such as the normalized vegetation index (NDVI) (Xu and Su, 2019) and the enhanced vegetation index (EVI) (Elmore et al., 2006). H_2 is determined by mapping the relationships between these vegetation indexes and groundwater depths while examining the variations in vegetation indexes as groundwater depths increase. Taking NDVI as an example, there are two relationships between NDVI and groundwater depths with the increase of groundwater depths (Dang et al., 2019). First, NDVI initially increases and then decreases with increasing groundwater depth. The groundwater depth corresponding to the maximum NDVI is identified as H_2 . Second, NDVI initially increases and then stabilizes with increasing groundwater depth. The groundwater depth corresponding to the stable NDVI is identified as H_2 . Given the diverse vegetation types and their distinct responses to groundwater depths in different ecosystems (e.g., grassland, woodland, wetland), the relationships between NDVI of different ecosystems and groundwater depths are mapped to determine H_2 .

This study takes a comprehensive approach by incorporating both soil properties and the actual growth states of vegetation to determine the groundwater depth threshold for preventing vegetation degradation. It introduces a synthetic method to calculate this threshold. During the growth period, if the ecological index of a specific grid is lower than the maximum ecological index observed during the non-growth period of that same grid, the vegetation growth state is deemed poor. In such cases, the groundwater depth threshold for preventing vegetation degradation is determined as the smaller value between H_1 and H_2 . Conversely, if the ecological index during the growth period exceeds the maximum ecological index during the non-growth period, the vegetation growth state is deemed satisfactory. Consequently, the groundwater depth threshold for preventing vegetation degradation is determined as larger value between H_1 and H_2 .

(2) Groundwater depth thresholds for preventing land subsidence

Land subsidence is influenced by various factors including groundwater depth, strata lithologic structure, hydrogeological conditions. In order to calculate the groundwater depth

threshold for preventing land subsidence, several methods are employed, all of which require the determination of an acceptable land subsidence depth. One approach involves analyzing long-term land subsidence observations, whether via land subsidence observation system or the remote sensing satellite to derive the statistical relationship between the groundwater depth decline and land subsidence, thereby determining the groundwater depth threshold for preventing land subsidence (Lu et al., 2022; Peng et al., 2022). Another method integrates groundwater dynamics with soil deformation modeling, facilitating the simulation of the stratum deformation caused by groundwater level declines, ultimately providing the groundwater depth threshold for preventing land subsidence (Ma & Luo, 2015). Furthermore, the layer-wise summation method (Equation 1) leverages geological and hydrogeological data to calculate the groundwater depth threshold for preventing land subsidence (Gong, 1996).

$$D = D_0 + S / \left(\mu_s \gamma \sum_{i=1}^n m_{vi} H_i \right) \quad (1)$$

where D is the groundwater depth threshold for preventing land subsidence, m; D_0 is the groundwater depth before the groundwater level decreases, m; S is the total land subsidence caused by the decline of groundwater level; μ_s is the land subsidence experience coefficient; γ is the bulk density of water, kN/kg; m_{vi} is the volume compression coefficient of layer i ; H_i is the thickness of layer i , m; n is the total number of layers.

(3) Groundwater depth thresholds for preventing Quaternary aquifer depletion

The Quaternary aquifer depletion is closely associated with groundwater exploitation. Many studies have highlighted the risk of aquifer depletion when the groundwater level experiences continuous decline or groundwater exploitation exceeds the allowable exploitable yield (Myriam et al., 2018; Sophocleous, 1997; Zhao et al., 2019). However, a consensus has not been reached regarding the specific threshold at which the groundwater level decline signifies aquifer depletion. This study assumes that the Quaternary aquifer is depleted when the groundwater depth exceeds two-thirds of the aquifer's thickness, which is defined as the groundwater depth threshold for preventing Quaternary aquifer depletion (Lu, 2020). Through borehole data analysis, it is possible to ascertain the thickness of Quaternary aquifer, thereby enabling the calculation of the groundwater depth threshold for preventing Quaternary aquifer depletion.

(4) The calculation of lower thresholds of the EGWD

By performing calculations to determine the groundwater depth thresholds for all protection targets, the minimum value among these thresholds for each grid is considered as the lower threshold of the EGWD.

2.3 Hydrological Model and Scenario Design

Accurately simulating long-term trajectories of groundwater depths is crucial for the sustainable evaluation of groundwater resources, especially considering the influence of climate change and/or human activities. Integrated surface water and groundwater models, such as HydroGeoSphere (Brunner & Simmons, 2012), SWAT-MODFLOW (Kim et al., 2008), GSFLOW (Markstrom et al., 2008), HEIFLOW (Tian, Zheng, Wu, et al., 2015; Tian, Zheng, Zheng, et al., 2015), prove to be effective tools for simulating hydrological cycle processes, including variations of the groundwater depth, groundwater flow movements, and interactions between surface water and groundwater. Importantly, the simulations should involve the potential effects of climate change and/or human activities on the groundwater depth. The Coupled Model Intercomparison Project Phase 6 (CMIP6), initiated by the World Climate Research Programme, provides access to meteorological data of multiple general circulation models (GCMs) and shared socioeconomic pathway (SSPs) developed by several research institutions around the world. Human activities significantly affect groundwater depth through land-use pattern changes and the implementation of water resources management measures. Examples include the conversion from drylands to paddies, the conversion from paddies to drylands, the alteration of the groundwater supply ratio, and exploitation scheduling. Incorporating these factors into simulations provides valuable insights for groundwater resource management.

2.4 Reliability, Resilience, and Vulnerability of Groundwater System

The sustainability evaluation of groundwater resources requires appropriate indexes to describe the characteristics of the groundwater depth exceeding threshold ranges of the EGWD. To determine the performance of the groundwater system, we adopt the RRV metrics, commonly used to evaluate water scarcity in water supply systems (Cai et al., 2002; Hashimoto et al., 1982;

McMahon et al., 2006; Sandoval-Solis et al., 2011; Zhang et al., 2017). RRV is used to describe the frequency, duration, and extent of the system being in an unsatisfactory state. In this study, RRV indexes are used to evaluate the sustainability performance of groundwater system by simulating the variations of groundwater depths under different scenarios.

Reliability represents the probability of a system being in a satisfactory state (Hashimoto et al., 1982). Specifically, reliability is defined as the ratio of the periods during which groundwater depths remain within threshold ranges of the EGWD to the total simulation periods. A higher reliability value indicates a more sustainable groundwater system.

$$\alpha = \frac{1}{n} \sum_{t=1}^n Z_t \quad (2)$$

where α is the reliability; n is the total number of simulation periods; t is the current period; Z_t is the status of the current period. Z_t equals 1 with the groundwater system being in a satisfactory state, otherwise Z_t equals 0.

Resilience represents the duration for a system to recover to the satisfactory state from an unsatisfactory state (Hashimoto et al., 1982). In our study, resilience is defined as the reciprocal of the longest duration of groundwater depths exceeding threshold ranges of the EGWD during the simulation period (Moy et al., 1986). A larger resilience value indicates a more resilient system, as it signifies a shorter duration for groundwater depths to return to threshold ranges of the EGWD and attain a satisfactory state.

$$\beta = \frac{1}{\text{MAX}(A_i)} \quad (3)$$

where β is the resilience; A_i is the duration of i th consecutive unsatisfactory state. When the groundwater depth is in the threshold range of the EGWD in all simulation periods, β equals 1.

Vulnerability represents the extent to which a system is deviates from a satisfactory state (Hashimoto et al., 1982). In our study, vulnerability is specifically defined as the maximum value of groundwater depth exceeding threshold ranges of the EGWD throughout the simulation period. To ensure comparability and account for variations in the EGWD across different areas and time periods, vulnerability is nondimensionalized and normalized following the approach suggested by Loucks (1997) and McMahon et al. (2006). A smaller normalized vulnerability value indicates a more sustainable groundwater system, signifying a lower extent of groundwater depths exceeding threshold ranges of the EGWD.

$$\gamma = \frac{\max(GWD_t - L_m)/L_m - \min(\max(GWD_t - L_m)/L_m)}{\max(\max(GWD_t - L_m)/L_m) - \min(\max(GWD_t - L_m)/L_m)} \quad (4)$$

where γ is the nondimensionalized and normalization vulnerability. GWD_t is the groundwater depth in period t ; m is the 12 months of the year; L_m is the monthly threshold of the EGWD.

3 Case Study

The lower reach of Tao'er River Basin (LTRB) in northeast China, with an area of 5,900 km², is selected as the study area (Figure 3). The average annual precipitation is 386.6 mm, the average annual evaporation is 1,091.4 mm, and the average annual temperature is 5.8 °C. Geomorphologically, the area primarily comprises of piedmont inclined plains and low plains. The piedmont inclined plain is distributed in the Tao'er River alluvial fan, while the low plain with the flat terrain is distributed in the eastward of alluvial fan. The lithology of the Quaternary pore phreatic aquifers in the river valley, alluvial fan, and low plain is predominantly composed of Holocene alluvial sand gravel, Pleistocene alluvial sand gravel, Pleistocene alluvial sand gravel, alluvial and lacustrine fine sand, and silky fine sand (Li et al., 2021).

The fragile eco-environment in the LTRB is highly susceptible to climate change and human activities. From 1990 to 2000, the farmland area increases from 2,972 to 10,872 km², with an increase of about 20%, among which the paddy area increases from 139 to 871 km², with an increase of over five times. The irrigation accounts for more than 80% of the total water consumption, leading to a substantial surge in water demand due to the increased agricultural land. The irrigation is dominated by groundwater, which accounts for more than 80% of the irrigation. Tens of thousands of pumping wells drilled for irrigation leads to continuous decline in regional groundwater levels. Previous reports (SRWRC, 2017; WRMC & WCSDI, 2015) have highlighted that the actual groundwater exploitation within the LTRB far exceeds the permissible exploitable yield, leading to groundwater depletion. This is further evidenced by the decline in groundwater levels, which are more than 2 m below the streambed elevation, indicating that the stream has been disconnected from groundwater in the LTRB (Ma et al., 2022; Wang et al., 2014). The vast stream leakage to groundwater, coupled with the impact of a series of droughts, results in frequent streamflow drying up events, which poses a significant threat to the health of river ecosystem. Furthermore, soil salinization has been observed in the southwest LTRB due to shallow

groundwater depths and strong groundwater evaporation rates. Consequently, there is an urgent need to investigate whether groundwater depths exceed threshold ranges of the EGWD for the sustainable groundwater exploitation within the LTRB.

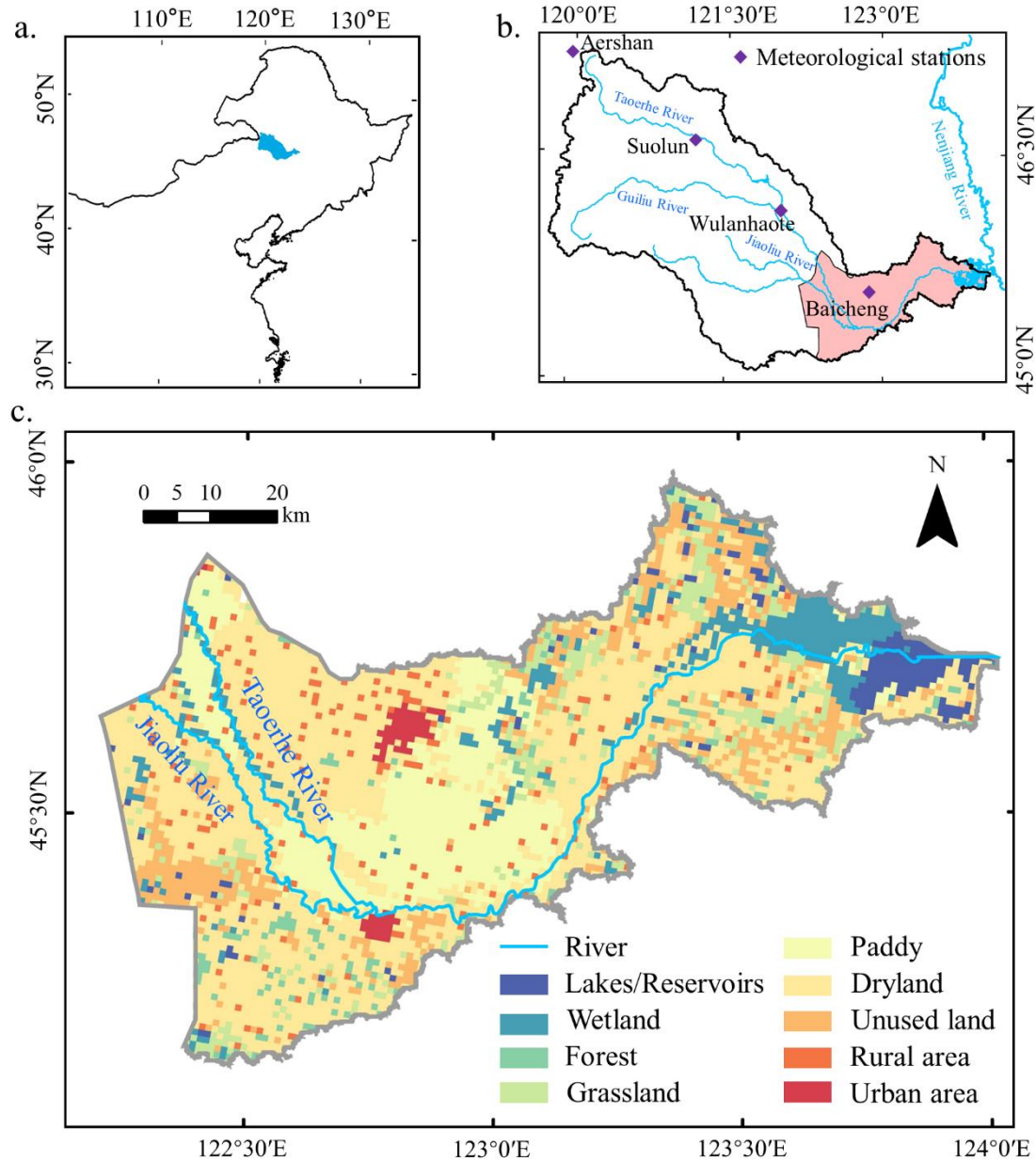


Figure 3 The study domain. (a) The location of the Tao'er River Basin; (b) The location of the LTRB; (c) The land-use in the LTRB. Reasons for selecting the LTRB as the study domain are as follows. First, groundwater overdraft resulting in various eco-environmental issues, mainly occurs in the LTRB, which is a crucial region to investigate the sustainability of groundwater resources. Second, there are adequate boreholes and groundwater level observations for establishing groundwater model in the LTRB. Third, the groundwater model is more suitable for the simulation

of the movements of the loose rock pore groundwater, which is mainly distributed in the LTRB.

The methods presented in Section 2.2 are used for calculating the EGWD in the LTRB. The upper threshold of the EGWD is determined by considering capillary rise heights specific to different soils and vegetation root depths in various ecosystems. On the other hand, the lower threshold of the EGWD takes into account three protection targets: vegetation degradation, land subsidence, and Quaternary aquifer depletion. The reasons are as follows. First, high-intensity groundwater extraction in the LTRB has led to a regional decline in groundwater levels, causing insufficient water supply for vegetation and subsequent degradation. Moreover, the decline of groundwater level transfers pressure to soil particles, posing a risk of land subsidence. Lastly, the Quaternary aquifer, primarily exploited for groundwater, serves as a crucial storage reservoir, with good water storage conditions, necessitating the prevention of depletion due to overexploitation. Detailed descriptions of data and methods for calculating the EGWD are presented in Table 1.

Table 1 The descriptions of data and methods for calculating the EGWD in the LTRB.

Types of the EGWD	Protection targets	Descriptions
Upper thresholds	Soil salinization and the growth of non-aquatic vegetation	Capillary rise heights of different soils (Supplementary Figure S1) are obtained from experimental results in Zhao (2012), and empirical values in CGS (2012). Vegetation root depths of paddy, dryland, grassland and woodland ecosystems are obtained referring to the field investigation results in Lu (2020) and Zhao (2012) and the empirical values in Chen (2001) and Yu (2003).
Lower thresholds (the shallowest of D ₁ , D ₂ , and D ₃)	Vegetation degradation (D ₁)	Extreme evaporation depths of different soils are obtained referring to calculation results in Fan (2004) and Zhao (2012) and empirical values in CGS (2012). NDVI is selected as the ecological indicator of vegetation growth state. Monthly NDVI from 2001 to 2016 is obtained from Resources and Environmental Science and Data Center, Institute of Geographic Sciences and Natural Resources Research, Chinese Academy of Sciences (https://www.resdc.cn).
	Land subsidence (D ₂)	The layer-wise summation method described in Section 2.2.2 is used to calculate the groundwater depth threshold for preventing land subsidence. S is 20 mm (Lu, 2020). μ_s and m_{vi} is 0.4 and 0.025 MPa ⁻¹ , respectively, referring to Chang (1990).
	Quaternary aquifer depletion (D ₃)	The thickness of Quaternary aquifer is obtained according to the borehole data, two-thirds of which is taken as the groundwater depth threshold for preventing Quaternary aquifer depletion (Lu, 2020).

An integrated SWAT-MODFLOW model is developed for the simulation of groundwater depths. The SWAT model encompasses the whole Tao'er River Basin and is driven by daily meteorological data, including precipitation, maximum and minimum temperature, wind speed, and solar radiation data at four weather stations (Figure 3b), covering the period from 1990 to 2016. The period is divided into the warm-up period (1990 - 1992), calibration period (2005 - 2016), and validation period (1993 - 2004). The MODFLOW model, focusing on the LTRB, employs uniform $1 \text{ km} \times 1 \text{ km}$ grids to discretize the Quaternary pore aquifer. The modelling domain, containing 5903 active grids, is generalized as a layer of unequal thickness, isotropic two-dimensional unsteady flow aquifer according to the borehole data. The streambed leakage, precipitation infiltration, and phreatic evaporation are obtained from SWAT model, and then transmitted to Visual MODFLOW through River Module, Recharge Module, and Evapotranspiration Module for groundwater simulation. The MODFLOW model is run with 10-day stress period from 2001 to 2016. The first eight years (2001 - 2008) are considered as the calibration period, and the remaining eight years (2009 - 2016) are used for validation. Further details regarding the setup, calibration, and validation of the integrated SWAT-MODFLOW can be found in our previous study (Wang et al. 2023). Monthly simulation results of integrated SWAT-MODFLOW model are used to calculate RRV.

For scenario design, we consider the impact of climate change on groundwater depths and assume that historical human activities will not change in the future. This is due to the fact that there were no major changes in land-use and groundwater supply and exploitation practices in the LTRB over the past two decades. Meteorological data, including daily precipitation, daily maximum and minimum temperature, from 5 GCMs and 3 SSPs, are obtained from CMIP6. Combined with historical meteorological data, a total number of 16 scenarios are designed (Table 2). Future meteorological data exhibit lower spatial resolution and deviations compared to historical data, necessitating spatial downscaling and deviation correction. The historical daily meteorological data from four weather stations (Figure 3b) serve as a reference for the correction process. First, the inverse distance weight method (Chaplot et al., 2006) is used to downscale the future gridded meteorological data to the four weather stations. Second, the quantile mapping method (Wilcke et al., 2013) is applied to modify the biased meteorological data. All scenarios'

meteorological data are fed into the integrated SWAT-MODFLOW model to simulate groundwater depths, and simulation results from 5 GCMs of the same emission scenario are as a set to calculate RRV.

Table 2 The climate scenarios characterized by various Shared Socioeconomic Pathways (SSPs) and General Circulation Models (GCMs).

Scenario	SSPs	GCMs	Time Range (Resolution)	Spatial Resolution
S0	History	-	1969-2016 (daily)	4 stations
S1	SSP126	BCC-CSM2-MR	2015-2064 (daily)	1.125°×1.125°
S2		GFDL-ESM4		1.250°×1.000°
S3		IPSL-CM6A-LR		2.500°×1.268°
S4		MPI-EMS1-2-LR		1.875°×1.875°
S5		MRI-ESM2-0		1.125°×1.125°
S6	SSP245	BCC-CSM2-MR		1.125°×1.125°
S7		GFDL-ESM4		1.250°×1.000°
S8		IPSL-CM6A-LR		2.500°×1.268°
S9		MPI-EMS1-2-LR		1.875°×1.875°
S10		MRI-ESM2-0		1.125°×1.125°
S11	SSP585	BCC-CSM2-MR		1.125°×1.125°
S12		GFDL-ESM4		1.250°×1.000°
S13		IPSL-CM6A-LR		2.500°×1.268°
S14		MPI-EMS1-2-LR		1.875°×1.875°
S15		MRI-ESM2-0		1.125°×1.125°

4 Results

4.1 Ecological Groundwater Depth in the LTRB

Upper and lower thresholds of the EGWD demonstrate notable spatial heterogeneity and temporal variability (Figure 4). Upper thresholds of the EGWD range from 1.16 to 2.05 meters during the non-growth period, with a majority of grids displaying values below 2 meters (Figure 4a). Upper thresholds of the EGWD range from 1.16 to 4.05 meters during the growth period, with most grids maintaining values below 3 meters (Figure 4b). Grids with larger upper thresholds of the EGWD are mainly covered with woodlands, where the vegetation roots are more developed and rooted deeper. On the other hand, lower thresholds of the EGWD range from 6.28 to 33.54

420 meters during the non-growth period (Figure 4c) and from 4.87 to 30.72 meters during the growth
421 period (Figure 4d), with the majority of grids exhibiting values below 20 meters. Lower thresholds
422 of the EGWD in the middle and border grids of the LTRB are deeper than 15 meters. In contrast,
423 grids in the south, western river valley, and wetlands have shallow lower thresholds of the EGWD,
424 which is less than 10 meters. These spatial and temporal dynamics in EGWD thresholds
425 underscore the influence of local vegetation characteristics and hydrogeological conditions on
426 groundwater depth variations.

427 During the non-growth period, the mitigation of soil salinization is the primary protection
428 target for upper thresholds of the EGWD, which is controlled by both the mitigation of soil
429 salinization and the facilitation of optimal growth of non-aquatic vegetation species during the
430 growth period. Lower thresholds of the EGWD are spatially controlled by different protection
431 targets (Figure 4e and 4f). In southwest grids, the prevention of Quaternary aquifer depletion, due
432 to its thin thickness, emerges as the prominent target during the non-growth period. Conversely, in
433 other grids, the prevention of land subsidence remains the primary target. During the growth
434 period, the preservation of vegetation becomes a dominant target in grasslands, wetlands, and
435 forests, while the protection targets in remaining grids align with those observed during the non-
436 growth period.

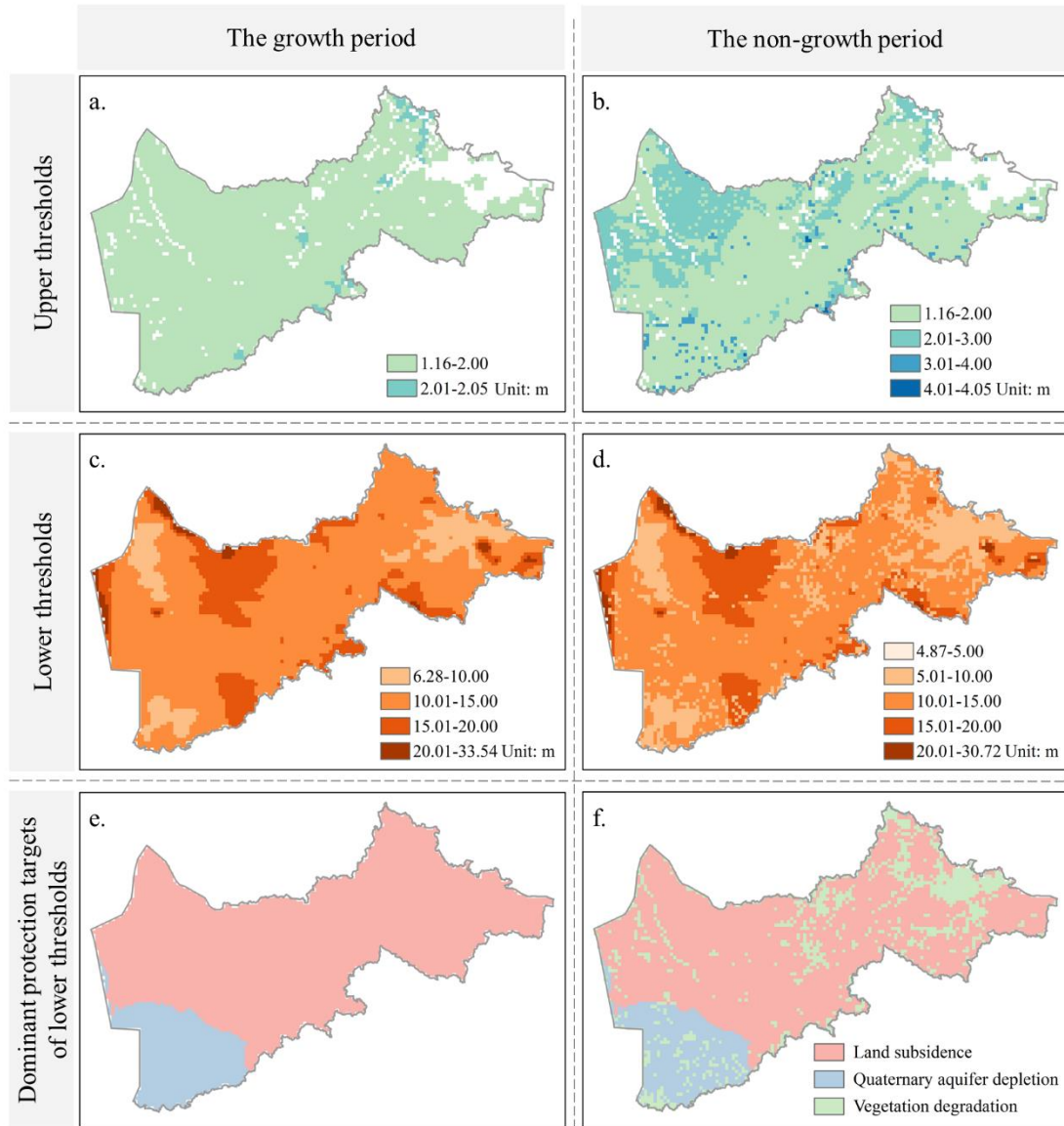


Figure 4 Ecological groundwater depths and their dominant protection targets in the LTRB. (a)-(b) Upper thresholds of the EGWD during the non-growth period and growth period, respectively. (c)-(d) Lower thresholds of the EGWD during the non-growth period and growth period, respectively. (e)-(f) Dominant protection targets that control lower thresholds of the EGWD in different grids during the non-growth period and growth period, respectively.

4.2 Reliability, Resilience, and Vulnerability of Groundwater System

There are more areas where groundwater depths exceed threshold ranges of the EGWD in future climate scenarios, as indicated by the increased presence of green areas compared to the historical scenario (Figure 5). In the historical, SSP126, SSP245, and SSP585 scenarios, areas

with reliability values less than 1.0 accounts for 26%, 41%, 44%, and 50%, respectively. Compared to the precipitation in the historical scenario, the projected precipitation in the SSP126, SSP245, and SSP585 scenarios shows an increase of 29%, 22%, and 29%, respectively. Meanwhile, the evapotranspiration is increased by 31%, 25%, and 29% (Supplementary Figure S2). Combined with the effects of rainfall and evaporation, the average precipitation infiltration into groundwater is also increased by 24%, 14%, and 30% during the simulation period, respectively (Supplementary Figure S2). This enhanced infiltration raises the possibility of groundwater depths exceeding upper thresholds of the EGWD in areas with shallow groundwater depths, such as the river valley between the Tao'er River and Jiaoliu River and the southwestern LTRB. Specifically, we find that 20%, 11%, and 19% of the whole basin experience such a transition in the SSP126, SSP245, and SSP585 scenarios, respectively. On the other hand, due to the increased precipitation infiltration into groundwater, the proportion of the LTRB area with low reliability values (<0.8) is projected to be 11%, 15%, and 11% for the SSP126, SSP245, and SSP585 scenarios, respectively, all of which are lower than 16% observed in the historical scenario. These areas with increased reliability in the future climate scenarios are mainly concentrated in the central LTRB.

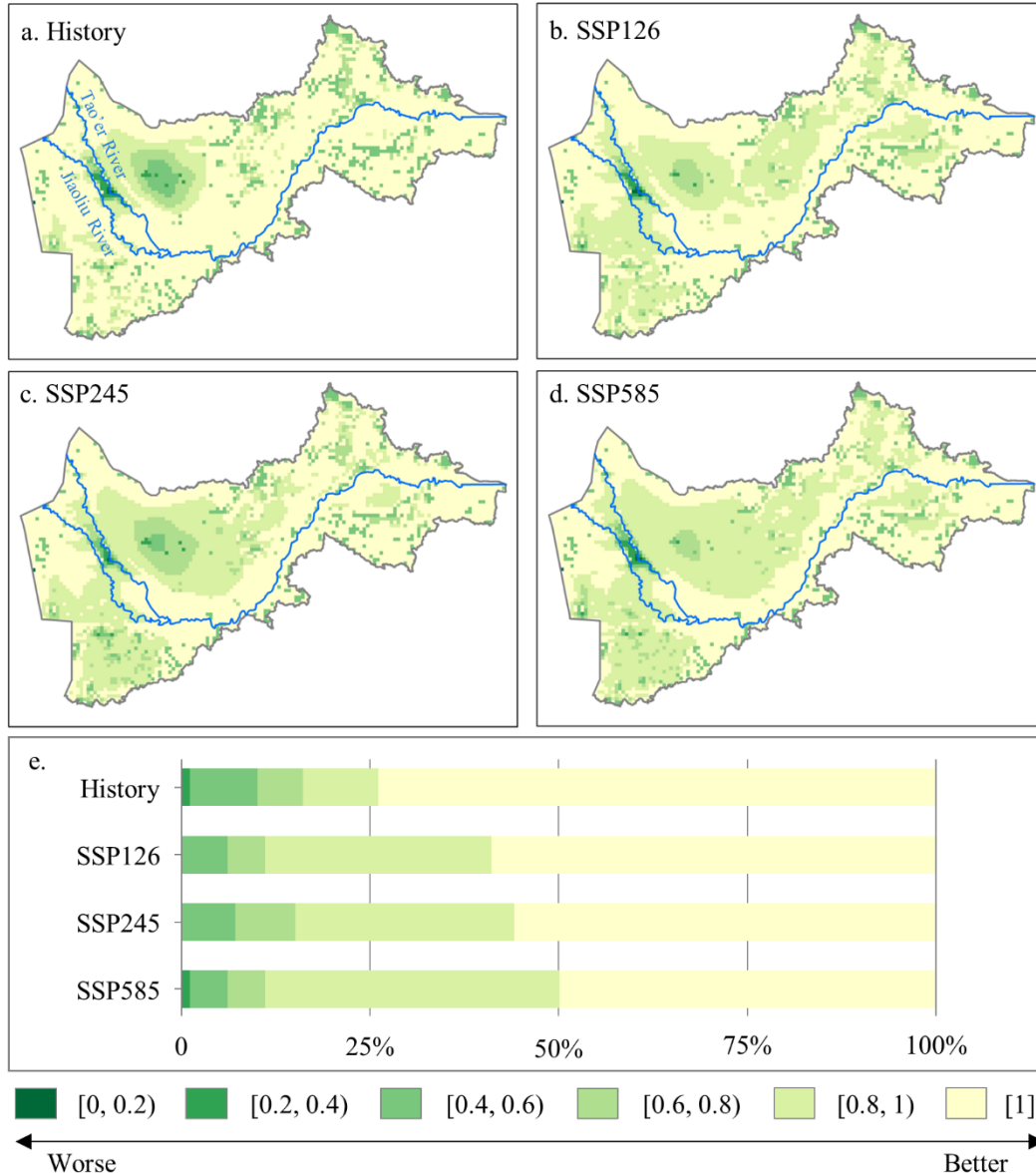


Figure 5 Reliability performances of groundwater system in the LTRB. Panels (a) to (d) present the spatial distribution of reliability values in the history, SSP126, SSP245, and SSP585 scenarios, respectively. Panel (e) presents the proportions of reliability values within different intervals.

Compared to the historical scenario, future climate scenarios exhibit poor resilience performances in the LTRB (Figure 6). The proportion of the LTRB area with resilience values less than 1/12 accounts for 8%, 17%, 22% and 26% in the historical, SSP126, SSP245, and SSP585 scenarios, respectively. This indicates a significant expansion of areas where groundwater depths exceed threshold ranges of the EGWD and fails to recover within one year. Unlike reliability that reflects the average performance of system during the simulation horizon, resilience reflects the

474 system performance during the extreme dry or wet events. In this study, for example, we define
475 the extreme dry or wet events as periods when the precipitation infiltration into groundwater falls
476 below or exceeds 25% of the average precipitation infiltration during the simulation stages.
477 Extreme dry events occurring in future climate scenarios exhibit longer durations compared to the
478 historical scenario (Supplementary Figure S3). Specifically, the historical scenario exhibits
479 extreme dry and wet periods less than 20 months and 10 months, respectively, while future
480 scenarios experience extreme dry and wet periods more than 30 months and 20 months,
481 respectively. In extreme dry periods, the reduction in precipitation infiltration into groundwater
482 makes the groundwater replenishment insufficient to compensate for the groundwater exploitation,
483 which results in prolonging the duration of groundwater depths exceeding threshold ranges of the
484 EGWD in the central and southern LTRB. Furthermore, extreme wet periods contribute to the
485 decreased resilience of groundwater depths exceeding upper thresholds of the EGWD in the river
486 valley between Tao'er River and Jiaoliu River and southwestern LTRB.

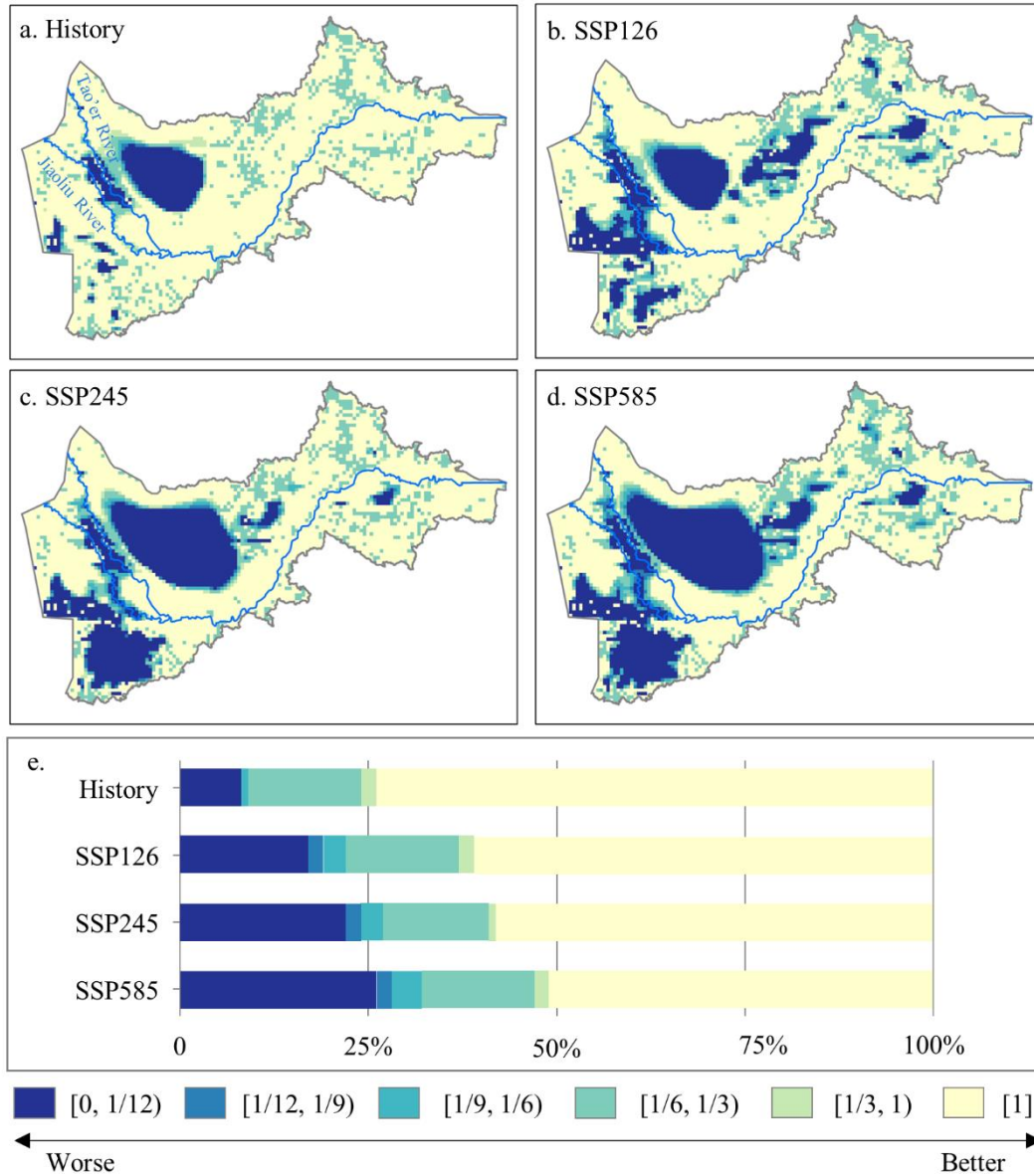


Figure 6 Resilience performances of groundwater system in the LTRB. Panels (a) to (d) present the spatial distributions of resilience values in the history, SSP126, SSP245, and SSP585 scenarios, respectively. Panel (e) presents the proportions resilience values within different intervals. The legend number, such as 1/12, indicates consecutive 12-month durations during which the groundwater depth exceeds the upper or lower thresholds of the EGWD, with similar implications conveyed by the numbers 1/3, 1/6, and 1/9.

In comparison to the historical scenario, future climate scenarios exhibit poorer vulnerability performances in the LTRB (Figure 7). Areas with vulnerability values below 0.2 accounts for 95%, 89%, 90% and 88% of the LTRB in the historical, SSP126, SSP245, and SSP585 scenarios.

The distribution of areas with high vulnerability has undergone a shift between the historical and future climate scenarios. In the historical scenario, the river valley between Tao'er River and Jiaoliu River exhibits high vulnerability values, whereas this issue is alleviated in future climate scenarios. The southern and eastern LTRB encounter scattered areas with high vulnerability values in the historical scenario, but grids with high vulnerability in these areas increase and cluster in future climate scenarios. Vulnerability, similar to resilience, represents the performance during an extreme dry or wet period. As mentioned above, although there is an overall increase in precipitation infiltration in future climate scenarios, the duration of extreme drought events becomes longer. It indicates that the cumulative drought intensity of single extreme drought event in future climate scenarios exceeding that in the historical scenario (Supplementary Figure S3). Enhanced extreme drought events lead to deeper groundwater depths in future climate scenarios. For example, in the southern LTRB, future climate scenarios depict the deepest groundwater depth approximately 6 meters below the lower threshold of the EGWD, which is about 2 m in the historical scenario. Analogously, the prolonged duration of extreme wet conditions in future climate scenarios increases the intensity of groundwater recharge, rising groundwater levels. For example, in some grids of eastern LTRB, the shallowest groundwater depth exceeds the upper threshold of the EGWD by about 1 m during extreme wet events in future climate scenarios, while it remains in the threshold range of the EGWD in the historical scenario.

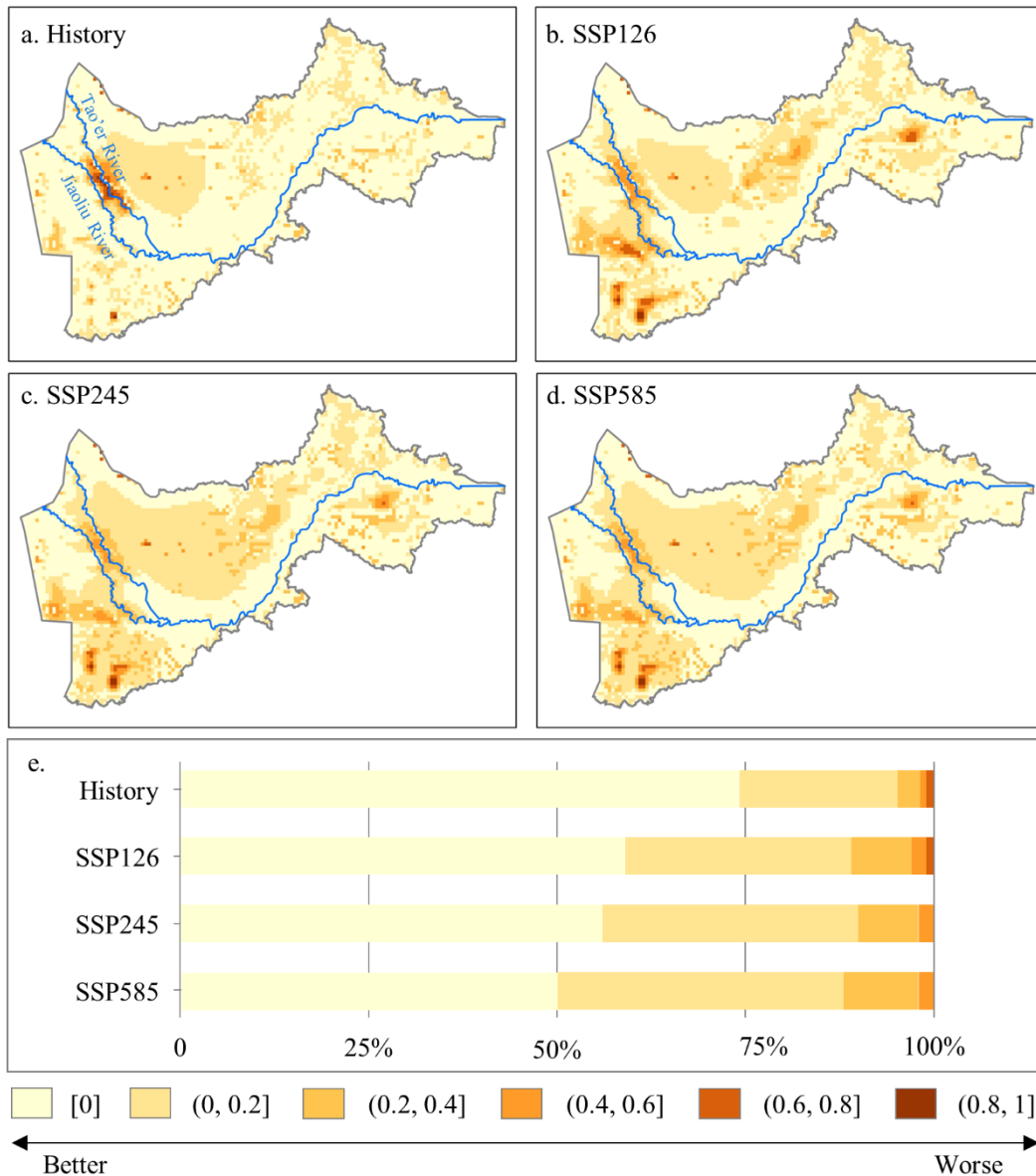


Figure 7 Vulnerability performances of groundwater system in the LTRB. Panels (a) to (d) present the spatial distribution of vulnerability values in the history, SSP126, SSP245, and SSP585 scenarios, respectively. Panel (e) presents the proportions of vulnerability values within different intervals.

4.3 Sustainability of Groundwater Resources in Some Key Subbasins

There is an expansion of areas experiencing groundwater resource unsustainability in future climate scenarios, primarily concentrated in regions I, II, and III (Figure 8). The criterion employed in this study to determine the sustainability of groundwater resources is based on the comprehensive performance of reliability, resilience and vulnerability metrics. Specifically, when

the reliability index falls below 0.8, resilience is less than 1/12, or vulnerability surpasses 0.2, it is suggested that the sustainability of groundwater resources becomes compromised. The expansion of areas experiencing groundwater resource unsustainability can be predominantly attributed to poor performances of resilience and vulnerability during extreme dry and wet periods (Figure 6 and 7).

Distinct challenges regarding the sustainability of groundwater resources are observed across various regions. Some areas face the specific issue of groundwater depths surpassing either the upper or lower threshold of EGWD, while others encounter both situations intermittently during different periods (Figure 8). In regions I and II, the unsustainability of groundwater resources can be chiefly attributed to groundwater depths falling below lower thresholds of the EGWD. The extent of groundwater resource unsustainability in the SSP126 scenario closely resembles that of the historical scenario. Whereas the SSP245 and SSP585 scenarios exhibit an expanding scope of this issue. In these scenarios, the duration of extreme dry periods exceeds 40 months and even reaches 65 months in the SSP585 scenario, compared to only 20 months in the historical scenario. The cumulative drought intensity of single extreme drought event in future climate scenarios surpasses that of the historical scenario (Supplementary Figure S3), resulting in poorer resilience and vulnerability performances. Moreover, in region II, the prevention of Quaternary aquifer depletion, due to its thin thickness, emerges as the prominent control target (Figure 4e and 4f). The groundwater depth is prone to decline rapidly when the groundwater exploitation occurs. Therefore, except for the impact of extreme drought, poor water-abundance is another reason for groundwater depths falling below lower thresholds of the EGWD.

The unsustainability of groundwater resources in regions III primarily stems from groundwater depths exceeding upper thresholds of the EGWD. The primary reason for the issue is the increased precipitation in future climate scenarios. Shallow groundwater depths, which are even less than 3 m in some areas (Supplementary Figure S4), also contribute to groundwater depths exceeding upper thresholds in this region. Soil salinization caused by shallow groundwater depths has been observed in region III. Furthermore, in the river valley of region III, the extensive leakage from the stream that replenishes groundwater serves as a significant factor in groundwater depths surpassing upper thresholds.

The LTRB is facing **dual challenges** of groundwater depletion and waterlogging.

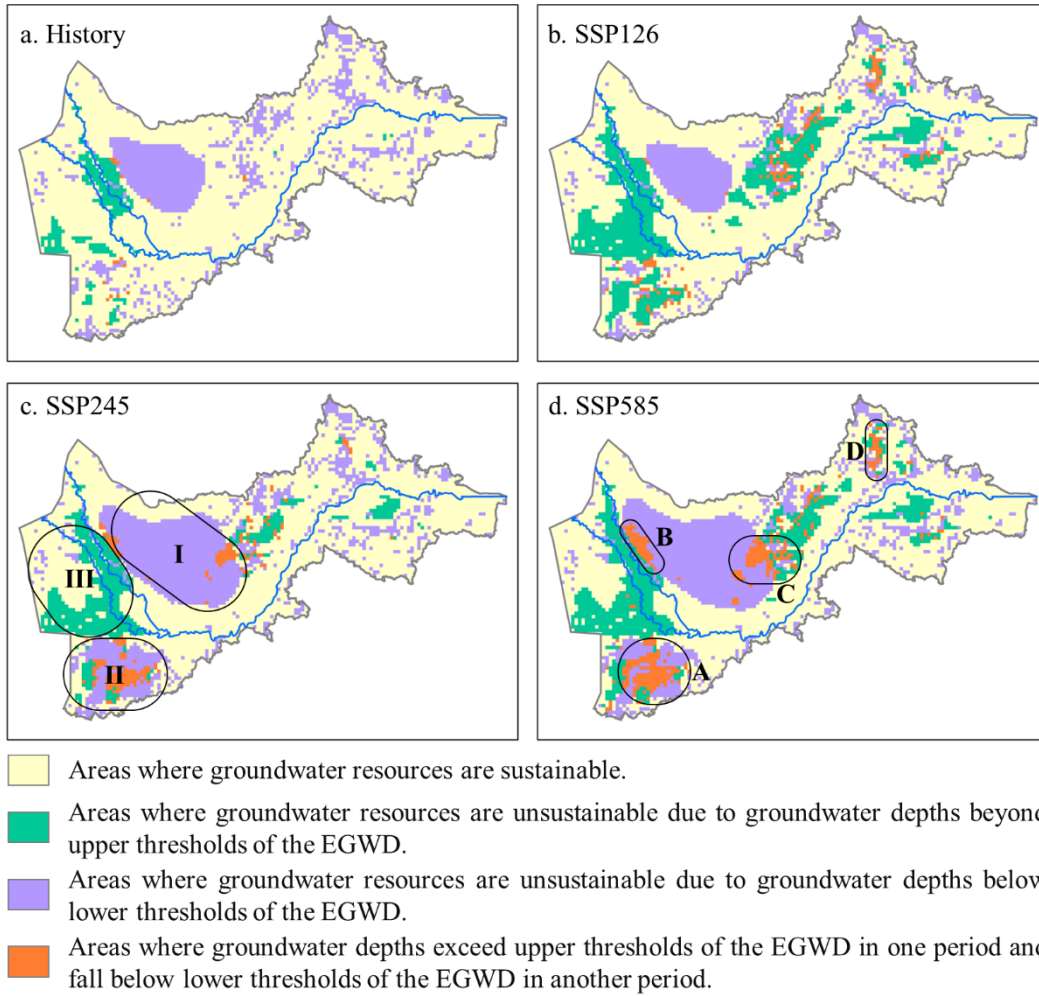


Figure 8 Spatial distributions of groundwater resource sustainability in (a) the history scenario, (b) the SSP126 scenario, (c) the SSP245 scenario, and (d) the SSP585 scenario.

Notably, certain areas have emerged where groundwater depths exceed upper thresholds of the EGWD in one period and fall below lower thresholds of the EGWD in another period. With the projected increase of anticipated emissions in future climate scenarios, the prevalence of such areas primarily intensifies within regions A, B, C, and D (Figure 8d). In scenario S0 (the historical scenario), groundwater depths have a high probability of falling below lower thresholds of the EGWD in four selected grids of regions A, B, C, and D (Figure 9). However, in scenario S15 (the MRI-ESM2-0 and SSP585 scenario), groundwater depths of regions A, C, and D rise and even exceed upper thresholds of the EGWD occasionally in the medium and long term (2037~2064) due to the climate transitioning towards wetter conditions. Groundwater depths in region B exceed

upper thresholds of the EGWD during the initial simulation years, then rapidly decrease to threshold ranges of the EGWD. Although region B does not experience groundwater depths falling below lower thresholds of the EGWD in scenario S15, the situation appears in scenarios S5 (the MRI-ESM2-0 and SSP126 scenario) and S6 (the BCC-CSM2-MR and SSP245 scenario) (Supplementary Figures S9b and S10b). Notably, in grids near the river in region B, there is a high probability of groundwater depths surpassing upper thresholds of the EGWD due to the leakage from the stream in the future (Supplementary Figure S19).

Climate change induces fluctuations of the intensity of precipitation infiltration recharge into groundwater during different periods in the future. The intensity of precipitation infiltration recharge into groundwater is initially weak in the near future and subsequently increase. This causes these areas encountering dual issues of groundwater depletion and waterlogging during different periods. This phenomenon is even more pronounced in the scenario of high emissions. Moreover, simulations of groundwater depth trajectories have certain variations in the same emission scenario, which are caused by uncertainties in future predictions of precipitation and temperature of different GCMs (Figure 9 and Supplementary Figures S5 – S18).

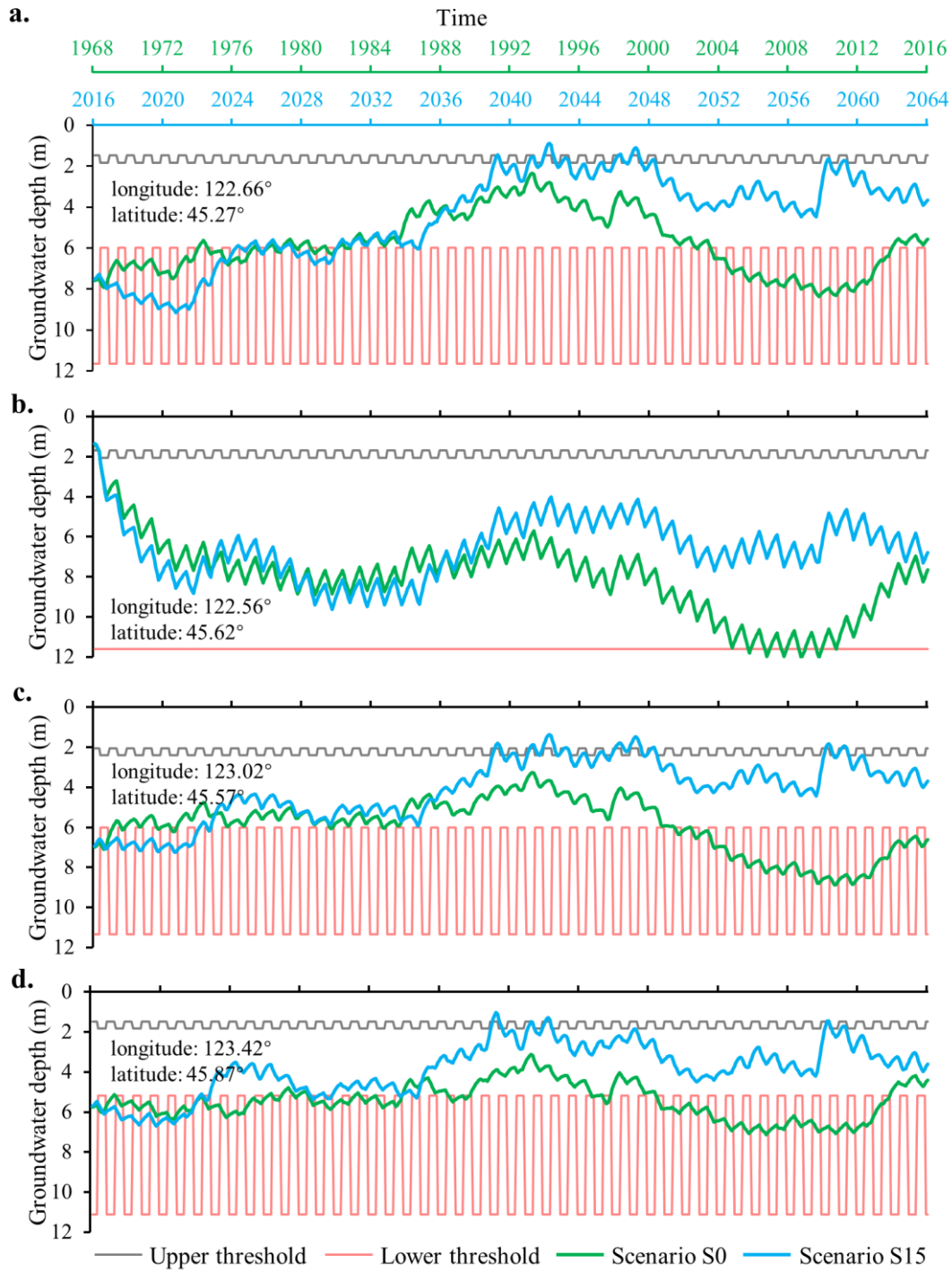


Figure 9 Projected trajectories of the groundwater depth in scenario S0 and scenario S15 in a grid at (a) region A, (b) region B, (c) region C, and (d) region D. The coordinates in the figure are the locations of the grids at region A, region B, region C, and region D. The results of other scenarios are displayed in Supplementary Figures S5 – S18.

5 Summary and Discussion

5.1 Summary

This paper develops a novel framework for evaluating the sustainability of groundwater resources. Assuming that the groundwater depth fluctuations resemble the operation of reservoirs, the framework utilizes the grid-scale dynamic EGWD considering multiple protective targets as the criterion to determine whether the groundwater depth remains within an appropriate range. To conduct a comprehensive evaluation of groundwater resource sustainability, the framework incorporates reliability, resilience, and vulnerability indexes to quantify the frequency, duration, and extent of groundwater depths exceeding threshold ranges of the EGWD. These quantifications are based on simulation results of an integrated surface water and groundwater model under multiple scenarios. By employing this framework, we can comprehensively assess risks associated with groundwater overexploitation and potential for groundwater resource utilization in different areas and periods. Moreover, it facilitates the identification of key areas that require focused attention in the future groundwater resources management efforts.

The proposed framework is applied to the LTRB located in Northeast China for evaluating the sustainability of groundwater resources under future climate change. The grid-scale dynamic EGWD considering 4 protective targets is calculated, and the dominated protected target is determined. During the non-growth period and growth period, upper thresholds of the EGWD exhibit a range of 1.16~2.05 meters and 1.16~4.05 meters, respectively, while lower thresholds of the EGWD show a range of 6.28~33.54 meters and 4.87~30.72 meters, respectively. Long-term trajectories of groundwater depths are simulated using an integrated SWAT-MODFLOW model under 16 historical and future climate scenarios. The results show that increased precipitation in future climate scenarios improves the reliability performance in areas with deep groundwater depths. However, it also increases the possibility of groundwater depths exceeding upper thresholds of the EGWD in areas with shallow groundwater depths. Notably, changes in future climate conditions lead to longer duration and greater intensity of extreme dry and wet events compared to the historical scenario. In the historical scenario, extreme dry and wet events last less than 20 months and 10 months, respectively. While in future climate scenarios, these extreme

events extend beyond 30 months for dry periods and 20 months for wet periods. Consequently, the cumulative intensity of single extreme climate event in future climate scenarios exceeds that of the historical scenario. It causes a significant expansion of areas experiencing poor performances of resilience and vulnerability indicators in future climate scenarios. These findings indicate that even with an increase in average precipitation in the future, extreme climate conditions give rise to different issues of groundwater depletion and waterlogging in different regions. Moreover, climate change induces fluctuations of the intensity of precipitation infiltration recharge into groundwater during different periods in the future, which causes dual challenges of groundwater depletion and waterlogging during different periods in some regions. This phenomenon is even more pronounced in the scenario of high emissions. Overall, these results highlight the significant challenges faced in managing groundwater resources in the future, emphasizing the importance and urgency of effective groundwater resource management in the LTRB.

5.2 Implications for regional groundwater resource management

There are significant challenges to the sustainability of groundwater resource management in the LTRB under future climate change. The proposed framework in this paper enables the evaluation of overexploitation risks and exploitation potential of groundwater resources in different areas and periods under the impacts of climate change, and facilitates the identification of key areas for future groundwater resource management. Our results provide some implications to facilitate informed decision-making and enable effective measures to be implemented in managing groundwater resources in the future.

There is a significant need for the groundwater management sector to enhance its capacity to address extreme climate conditions. Although the reliability performance of groundwater system improves due to the increased precipitation in future climate scenarios, extreme climate events lead to poorer performances of resilience and vulnerability compared to the historical scenario (Figures 5~7). In the context of impending climate changes, extreme climate conditions impose more stringent demands on groundwater resource management (Candela et al., 2012; Le Brocq et al., 2018), which is vital for ensuring regional security of water supply, food and ecology (Liu et al., 2022; Pagán et al., 2016; Yan et al., 2014).

Optimizing the crop planting structure can be an effective measure to achieve spatially sustainable groundwater exploitation (Luo et al., 2022). In the LTRB, where the unsustainability of groundwater resources is observed due to groundwater depths exceeding threshold ranges of the EGWD (Figure 8), the predominant land use is cultivated land, with groundwater irrigation accounting for over 80% of the total water supply. This indicates that the crop planting structure plays a significant role in determining the spatial patterns of groundwater exploitation. Implementing a conversion from paddies to drylands in areas with high-intensity groundwater exploitation and a tendency for groundwater depths to fall below the lower threshold of the EGWD, such as region I, can increase the groundwater level. Implementing a conversion from drylands to paddies in areas with low-intensity groundwater exploitation and shallow groundwater depths, where groundwater depths are likely to exceed upper thresholds of the EGWD, such as region III, can decrease the groundwater level. This highlights the importance of considering the spatial optimization of crop planting structure as a strategy to achieve sustainable groundwater exploitation. By implementing appropriate land use changes, it is possible to mitigate the challenges associated with groundwater unsustainability and promote the long-term viability of groundwater resources.

Taking a long-term perspective, it is crucial to manage groundwater exploitation in a manner that makes full use of the regulation and storage capacity of the aquifer. If the historical groundwater exploitation scheduling continues to be implemented in future climate scenarios, there are areas experiencing dual issues of groundwater depletion and waterlogging during different periods (Figures 8 and 9). To address these challenges, it is necessary to implement different measures during different periods in the future. In the near future, groundwater resource management measures should be implemented to mitigate the risk of groundwater depths falling below the lower thresholds of the EGWD. In the medium term, measures should be taken to prevent the risk of groundwater depths exceeding the upper thresholds of the EGWD. Additionally, continuous monitoring of groundwater dynamics is essential to maintain groundwater depths within the threshold ranges of the EGWD in the long run. While it will make the management of groundwater resources more challenges, it is important to recognize that the aquifer, that is, groundwater reservoir, possesses strong interannual regulation capabilities (Dai et

al., 2005). Therefore, it is necessary to manage groundwater exploitation from a long-term perspective, leveraging the aquifer's regulation and storage abilities to achieve rational groundwater exploitation over time.

5.3 Limitations and future work

A comprehensive exploration that considers the coupling impacts of both climate change and human activities on groundwater resources is crucial for a holistic understanding of groundwater system. The evaluation of groundwater resource sustainability in this study only focuses on the impact of future climate change. Although it can assist in formulating management measures for groundwater resources in the future, the growing prominence of human activities and their effects on groundwater resources are not considered in this study. By incorporating the effects of specific human activities, such as planting patterns (Wang, et al., 2022), irrigation system layouts (Shandany et al., 2018), and irrigation efficiency (Zhang et al., 2017), alongside climate change, a more accurate evaluation of groundwater resource sustainability can be achieved. Understanding the interplay between these factors and groundwater resources can establish a more robust and adaptive approach to groundwater resource management and ensure the long-term sustainability of this vital water source.

Acknowledgements

This work is supported by the National Natural Science Foundation of China (51925902 and 52009015).

Data availability

All the data used in this study are previously published and can be accessed. The monthly normalized vegetation index (NDVI) data can be obtained from Resources and Environmental Science and Data Center, Institute of Geographic Sciences and Natural Resources Research, Chinese Academy of Sciences (<https://www.resdc.cn>). Public data sets used to drive the integrated SWAT-MODFLOW model simulations are available via Geospatial Data Cloud site, Computer

Network Information Center, Chinese Academy of Sciences (<http://www.gscloud.cn>) (DEM),
Resources and Environment Science and Data Center, Chinese Academy of Sciences
(<http://www.resdc.cn>) (land-use map), National Cryosphere Desert Data Center (Lu & Liu, 2019)
(soil map), National Meteorological Information Center, China Meteorological Administration
(<http://data.cma.cn>) (precipitation, maximum and minimum temperature, relative humidity, wind
speed), Global Land Evaporation Amsterdam Model (Martens et al., 2017; Miralles et al., 2011)
(remote sensing evapotranspiration), and Coupled Model Intercomparison Project Phase 6
(CMIP6) (<https://esgf-node.llnl.gov/search/cmip6>) (future precipitation, maximum and minimum
temperature). Other data used to develop the integrated SWAT-MODFLOW model, including
river network, boreholes, surface water and groundwater extracts, streamflow observations, and
groundwater level observations, are available from the corresponding authors upon reasonable
request.

Author contributions

Bo Xu conceived the research. Mingjun Wang performed the research. Mingjun Wang, Bo
Xu, and Chi Zhang analyzed the results and drafted the manuscript. Yong Peng and Yu Li polished
the manuscript. Xinqiang Du constructed the ecological groundwater depth. Chi Zhang and Bing
Yu provided funding support.

Competing interests

The authors declare no competing interests.

Additional information

Correspondence and requests for materials should be addressed to Bo Xu
(xubo_water@dlut.edu.cn).

References

Alley, W., Reilly, T. E., & Franke, O. L. (1999). Sustainability of Ground-Water Resources. *U.S.*

- 722 *Geological Survey Circular*, 1186.
- 723 Bierkens, M. F. P., & Wada, Y. (2019). Non-renewable groundwater use and groundwater
 724 depletion: A review. *Environmental Research Letters*, 14(6), 063002.
 725 <https://doi.org/10.1088/1748-9326/ab1a5f>
- 726 Brunner, P., & Simmons, C. T. (2012). Hydrogeosphere: a fully integrated, physically based
 727 hydrological model. *Groundwater*, 50(2). <https://doi.org/10.1111/j.1745-6584.2011.00882.x>
- 728 Bui, N. T., Kawamura, A., Amaguchi, H., Bui, D. D., Truong, N. T., & Nakagawa, K. (2018).
 729 Social sustainability assessment of groundwater resources: A case study of Hanoi, Vietnam.
 730 *Ecological Indicators*, 93, 1034-1042. <https://doi.org/10.1016/j.ecolind.2018.06.005>
- 731 Cai, X., Mckinney, D. C., & Lasdon, L. S. (2002). A framework for sustainability analysis in water
 732 resources management and application to the Syr Darya Basin. *Water Resources Research*,
 733 38(6), 1085. <https://doi.org/10.1029/2001WR000214>
- 734 Candela, L., Elorza, F. J., Jiménez-Martínez, J., & von Igel, W. (2012). Global change and
 735 agricultural management options for groundwater sustainability. *Computers and Electronics
 736 in Agriculture*, 86, 120-130. <https://doi.org/10.1016/j.compag.2011.12.012>
- 737 Chaplot, V., Darboux, F., Bourennane, H., Leguedois, S., Silvera, N., & Phachomphon, K. (2006).
 738 Accuracy of interpolation techniques for the derivation of digital elevation models in relation
 739 to landform types and data density. *Geomorphology*, 77(1-2), 126-141.
 740 <https://doi.org/10.1016/j.geomorph.2005.12.010>
- 741 Chang, S. (1990). *Handbook of Engineering Geology*. Beijing: China Architecture & Building
 742 Press.
- 743 Chen, S. (2001). *Grassland Plant Roots in Northern China*. Changchun: Jilin University Press.
- 744 China Geological Survey (CGS). (2012). *Handbook of Hydrogeology (Second Edition)*. Beijing:
 745 Geology Press.
- 746 Dai, C., Chi, B., & Gao, S. (2005). Analysis and calculation of regulated water resources of
 747 groundwater reservoir. *Chinese Geographical Science*, 15(1), 60–63.
 748 <https://doi.org/10.1007/s11769-003-0070-z>
- 749 Dang, X., Lu, N., Gu, X., & Jin, X. (2019). Groundwater threshold of ecological vegetation in
 750 Qaidam Basin. *Hydrogeology and Engineering Geology*, 46(3), 1-8.

- 751 <https://doi.org/10.16030/j.cnki.issn.1000-3665.2019.03.01>
- 752 Dangar, S., Asoka, A., & Mishra, V. (2021). Causes and implications of groundwater depletion in
753 India: A review. *Journal of Hydrology*, 596, 126103.
754 <https://doi.org/10.1016/j.jhydrol.2021.126103>
- 755 Doll, P., Hoffmann-Dobrev, H., Portmann, F. T., Siebert, S., Eicker, A., Rodell, M., et al. (2012).
756 Impact of water withdrawals from groundwater and surface water on continental water
757 storage variations. *Journal of Geodynamics*, 59-60, 143-156.
758 <https://doi.org/10.1016/j.jog.2011.05.001>
- 759 Dong, B., Zhang, X., Li, X., & Zhang, D. (2008). Comprehensive tests on rising height of
760 capillary water. *Chinese Journal of Geotechnical Engineering*, 30(10), 1569-1574.
- 761 Duran-Llacer, I., Arumi, J. L., Arriagada, L., Aguayo, M., Rojas, O., Gonzalez-Rodriguez, L., et
762 al. (2022). A new method to map groundwater-dependent ecosystem zones in semi-arid
763 environments: A case study in Chile. *Science of the Total Environment*, 816, 151528.
764 <https://doi.org/10.1016/j.scitotenv.2021.151528>
- 765 Elmore, A. J., Manning, S. J., Mustard, J. F., & Craine, J. M. (2006). Decline in alkali meadow
766 vegetation cover in California: the effects of groundwater extraction and drought. *Journal of*
767 *Applied Ecology*, 43(4), 770-779. <https://doi.org/10.1111/j.1365-2664.2006.01197.x>
- 768 Famiglietti, J. S. (2014). The global groundwater crisis. *Nature Climate Change*, 4(11), 945-948.
769 <https://doi.org/10.1038/nclimate2425>
- 770 Fan, Z., Ma, Y., Zhang, H., Wang, R., Zhao, Y., & Zhou, H. (2004). Research of eco-water table
771 and rational depth of groundwater of Tarim River drainage basin. *Arid Land Geography*,
772 27(1), 8-13. <https://doi.org/10.13826/j.cnki.cn65-1103/x.2004.01.002>
- 773 Fu, Q., Zhang, J., & Wang, Q. Adapt ability study on empirical formulae of frequent phreatic
774 evaporation in Xinjiang. *Agricultural Research in the Arid Areas*, 26(3), 182-188.
- 775 Gejl, R. N., Rygaard, M., Henriksen, H. J., Rasmussen, J., & Bjerg, P. L. (2019). Understanding
776 the impacts of groundwater abstraction through long-term trends in water quality. *Water*
777 *Research*, 156, 241-251. <https://doi.org/10.1016/j.watres.2019.02.026>
- 778 Gong, X. (1996). *Advanced soil mechanics*. Hangzhou, Zhejiang University Press, 203-210.
- 779 Gorelick, S. M., & Zheng, C. (2015). Global change and the groundwater management challenge.

- 780 *Water Resources Research*, 51(5), 3031-3051. <https://doi.org/10.1002/2014WR016825>
- 781 Hashimoto, T., Stedinger, J. R., & Loucks, D. P. (1982). Reliability, resiliency, and vulnerability
- 782 criteria for water-resource system performance evaluation. *Water Resources Research*, 18(1),
- 783 14-20. <https://doi.org/10.1029/WR018i001p00014>
- 784 Huang, F., Zhang, Y., Zhang, D., & Chen, X. (2019). Environmental groundwater depth for
- 785 groundwater-dependent terrestrial ecosystems in arid/semiarid regions: A Review.
- 786 *International Journal of Environmental Research and Public Health*, 16(5), 763.
- 787 <https://doi.org/10.3390/ijerph16050763>
- 788 Le Brocque, A. F., Kath, J., & Reardon-Smith, K. (2018) Chronic groundwater decline: A multi-
- 789 decadal analysis of groundwater trends under extreme climate cycles. *Journal of Hydrology*,
- 790 561, 976-986. <https://doi.org/10.1016/j.jhydrol.2018.04.059>
- 791 Li, H., Wang, F., Liu, Y., Zhao, H., Bao, S., & Chang, K. (2021). Shallow groundwater level under
- 792 climate change conditions in the Tao'er River plain. *Journal of Beijing Normal University*
- 793 *(Natural Science)*, 57(3), 345-352. <https://doi.org/10.12202/j.0476-0301.2020349>
- 794 Liu, M., Guo, Y., Wang, Y., & Hao, J. (2022). Changes of Extreme Agro-Climatic Droughts and
- 795 Their Impacts on Grain Yields in Rain-Fed Agricultural Regions in China over the Past 50
- 796 Years. *Atmosphere*, 13(1), 4. <https://doi.org/10.3390/atmos13010004>
- 797 Loucks, D. P. (1997). Quantifying trends in system sustainability. *Hydrological Sciences Journal-*
- 798 *Journal Des Sciences Hydrologiques*, 42(4), 513-530.
- 799 <https://doi.org/10.1080/02626669709492051>
- 800 Lu, L., & Liu, C. (2019). Chinese soil data set based on world soil database (HWSD) (v1.1).
- 801 National Cryosphere Desert Data Center (<http://www.ncdc.ac.cn>).
- 802 Lu, Y., Song, Z., Liu, J., Bu, F., & Qi, C. (2022). Land subsidence monitoring and deformation
- 803 analysis of Tongzhou bay area based on DFOS. *Journal of Hohai University (Natural*
- 804 *Sciences)*, 51(02), 81-88. <https://doi.org/10.3876/j.issn.1000-1980.2023.02.011>
- 805 Lu, X. (2020). Analysis of sustainable development and utilization plan of groundwater resources
- 806 of Songhua River and Naoli River Basin in Sanjiang Plain, (Master's Thesis). Retrieved from
- 807 China National Knowledge Internet. (<https://doi.org/10.27162/d.cnki.gjlin.2020.002709>)
- 808 Changchun: Jilin University.

- Luo, J., Zhang, H., Qi, Y., Pei, H., & Shen, Y. (2022). Balancing water and food by optimizing the planting structure in the Beijing-Tianjin-Hebei region, China. *Agricultural Water Management*, 262, 107326. <https://doi.org/10.1016/j.agwat.2021.107326>
- Ma, Q., & Luo, Z. (2015). Numerical simulation of groundwater exploitation and land subsidence in Cangzhou City. *Water Resources Protection*, 31(4), 20-26. <https://doi.org/10.3880/j.issn.1004-6933.2015.04.004>
- Ma, Z., Wang, W., Zhang, Z., Philip, B., Wang, Z., Chen, L., et al. (2019). Assessing bare-soil evaporation from different water-table depths using lysimeters and a numerical model in the Ordos Basin, China. *Hydrogeology Journal*, 27(7), 2707-2718. <https://doi.org/10.1007/s10040-019-02012-0>
- Ma, Z., Wang, W., Zhao, M., Hou, X., Wang, Z., & Zheng, H. (2022). Non-Darcy flow through a natural streambed in a disconnected stream. *Water Resources Research*, 58, e2021WR031356. <https://doi.org/10.1029/2021WR031356>
- Malekinezhad, H., & Banadkooki, F. B. (2018). Modeling impacts of climate change and human activities on groundwater resources using MODFLOW. *Journal of Water and Climate Change*, 9(1), 156-177. <https://doi.org/10.2166/wcc.2017.147>
- Markstrom, S. L., Niswonger, R. G., Regan, R. S., Prudic, D. E., & Barlow, P.M. (2008). GSFLOW-Coupled Ground-water and Surface-water FLOW model based on the integration of the Precipitation-Runoff Modeling System (PRMS) and the Modular Ground-Water Flow Model (MODFLOW-2005): U.S. Geological Survey Techniques and Methods 6-D1, 240 p. <https://doi.org/10.3133/tm6D1>
- Martens, B., Miralles, D. G., Lievens, H., van der Schalie, R., de Jeu, R.A.M., Fernández-Prieto, D., Beck, H. E., Dorigo, W. A., & Verhoest, N. E. C. (2017). GLEAM v3: satellite-based land evaporation and root-zone soil moisture. *Geoscientific Model Development*, 10(5), 1903–1925. <https://doi.org/10.5194/gmd-10-1903-2017>
- Mays, L. W. (2013). Groundwater Resources Sustainability: Past, Present, and Future. *Water Resources Management*, 27(13), 4409-4424. <https://doi.org/10.1007/s11269-013-0436-7>
- McMahon, T. A., Adeloye, A. J., & Zhou S. (2006). Understanding performance measures of reservoirs. *Journal of Hydrology*, 324(1-4), 359-382.

<https://doi.org/10.1016/j.jhydrol.2005.09.030>

Meng, B., Liu, J. L., Bao, K., & Sun, B. (2019). Water fluxes of Nenjiang River Basin with ecological network analysis: Conflict and coordination between agricultural development and wetland restoration. *Journal of Cleaner Production*, 213, 933-943.

<https://doi.org/10.1016/j.jclepro.2018.12.243>

Metternicht, G. I., & Zinck, J. A. (2003). Remote sensing of soil salinity: Potentials and constraints. *Remote Sensing of Environment*, 85(5), 1-20. [https://doi.org/10.1016/S0034-4257\(02\)00188-8](https://doi.org/10.1016/S0034-4257(02)00188-8)

Miralles, D. G., Holmes, T. R. H., de Jeu, R. A. M., Gash, J. H., Meesters, A. G. C. A., & Dolman, A. J. (2011). Global land-surface evaporation estimated from satellite-based observations. *Hydrology and Earth System Sciences*, 15(2), 453–469. <https://doi.org/10.5194/hess-15-453-2011>

Moreira, L. C. J., Teixeira, A. D., & Galvao, L. S. (2015). Potential of multispectral and hyperspectral data to detect saline-exposed soils in Brazil. *GIScience and Remote Sensing*, 52(4), 416-436. <https://doi.org/10.1080/15481603.2015.1040227>

Moy, W. S., Cohon, J. L., & Reville, C. S. (1986). A programming-model for analysis of the reliability, resilience, and vulnerability of a water-supply reservoir. *Water Resources Research*, 22(4), 489-498. <https://doi.org/10.1029/WR022i004p00489>

Myriam, S. S., Ahmed, H. A., Omar, S., Francois, Z., & Ronald, J. (2018). Groundwater balance politics: Aquifer overexploitation in the Orontes River Basin. *Water Alternatives*, 11(3), 663-683.

Jia, L., Guo, Z., Long Y., Guo, K., & Liao, Z. (2015). Research advances in ecological groundwater level in arid areas. *Ecological Science*, 34(2), 187–193. <https://doi.org/10.14108/j.cnki.1008-8873.2015.02.028>

Kath, J., Boulton, A. J., Harrison, E. T., & Dyer, F. J. (2018). A conceptual framework for ecological responses to groundwater regime alteration (FERGRA). *Ecohydrology*, 11(7), e2010. <https://doi.org/10.1002/eco.2010>

Karimi, D., Bahrami, J., Mobaraki, J., Missimer, T. M., & Taheri, K. (2022). Groundwater sustainability assessment based on socio-economic and environmental variables: a simple

- dynamic indicator-based approach. *Hydrogeology Journal*, 30(7), 1963-1988.
<https://doi.org/10.1007/s10040-022-02512-6>
- Kim, N. W., Chung, I. M., Won, Y. S., & Arnold, J. G. (2008). Development and application of the integrated SWAT–MODFLOW model. *Journal of Hydrology*, 356(1-2), 1-16.
<https://doi.org/10.1016/j.jhydrol.2008.02.024>
- Konikow, L. F., & Kendy, E. (2005). Groundwater depletion: A global problem. *Hydrogeology Journal*, 13(1), 317-320. <https://doi.org/10.1007/s10040-004-0411-8>
- Kumar, P., Tiwari, P., Biswas, A., & Acharya, T. (2022). Geophysical investigation for seawater intrusion in the high-quality coastal aquifers of India: a review. *Environmental Science and Pollution Research*, 30(4), 9127-9163. <https://doi.org/10.1007/s11356-022-24233-9>
- Pagán, B. R., Ashfaq, M., Rastogi, D., Pal, J. S., Kao, S. C., Naz, B. S., Mei, R., & Pal, J. S. (2016). Extreme hydrological changes in the southwestern US drive reductions in water supply to Southern California by mid century. *Environmental Research Letters*, 11(9), 094026. <https://doi.org/10.1088/1748-9326/11/9/094026>
- Pan, J., Wang, Z., Liang, H., & Zhao, L. (2018). Study on groundwater ecological level around Shifosi Reservoir. *Water Resources and Power*, 36(6), 141-145.
- Pandey, V. P., Shrestha, S., Chapagain, S. K., Kazama, F. (2011). A framework for measuring groundwater sustainability. *Environmental Science and Policy*, 14(4), 396-407.
<https://doi.org/10.1016/j.envsci.2011.03.008>
- Peng, M., Lu, Z., Zhao, C., Motagh, M., Bai, L., Conway, B. D., & Chen, H. (2022). Mapping land subsidence and aquifer system properties of the Willcox Basin, Arizona, from InSAR observations and independent component analysis. *Remote Sensing of Environment*, 271, 112894. <https://doi.org/10.1016/j.rse.2022.112894>
- Ruan, Y., & Wu, X. (2022). Evaluation of groundwater resource sustainability based on GRACE and GLDAS in arid region of Northwest China. *Arid Zone Research*, 39(3), 787-800.
<https://doi.org/10.13866/j.azr.2022.03.12>
- Samani, S., Moghaddam, H. K., & Zareian, M. J. (2021). Evaluating time series integrated groundwater sustainability: a case study in Salt Lake catchment, Iran. *Environmental Earth Sciences*, 80(17), 603. <https://doi.org/10.1007/s12665-021-09888-w>

- 896 Sandoval-Solis, S., McKinney, D. C., & Loucks, D. P. (2011). Sustainability Index for water
897 resources planning and management. *Journal of Water Resources Planning and*
898 *Management-ASCE*, 137(5), 381-390. [https://doi.org/10.1061/\(ASCE\)WR.1943-](https://doi.org/10.1061/(ASCE)WR.1943-5452.0000134)
899 [5452.0000134](https://doi.org/10.1061/(ASCE)WR.1943-5452.0000134)
- 900 Scanlon, B. R., Fakhreddine, S., Rateb, A., de Graaf, I., Famiglietti, J., Gleeson, T., et al. (2023).
901 Global water resources and the role of groundwater in a resilient water future. *Nature*
902 *Reviews Earth & Environment*, 4(2), 87-101. <https://doi.org/10.1038/s43017-022-00378-6>
- 903 Shah, N., Nachabe, M., & Ross, M. (2007). Extinction depth and evapotranspiration from ground
904 water under selected land covers. *Ground Water*, 45(3), 329-338.
905 <https://doi.org/10.1111/j.1745-6584.2007.00302.x>
- 906 Shandany, S. M. H., Firoozfar, A., Maestre, J. M., Mallakpour, I., Taghvaeian, S., & Karimi, P.
907 (2018). Operational performance improvements in irrigation canals to overcome groundwater
908 overexploitation. *Agricultural Water Management*, 204, 234-246.
909 <https://doi.org/10.1016/j.agwat.2018.04.014>
- 910 Singh, A. (2014). Conjunctive use of water resources for sustainable irrigated agriculture. *Journal*
911 *of Hydrology*, 519, 1688-1697. <https://doi.org/10.1016/j.jhydrol.2014.09.049>
- 912 Singh, A. (2021). Soil salinization management for sustainable development: A review. *Journal of*
913 *Environmental Management*, 277, 111383. <https://doi.org/10.1016/j.jenvman.2020.111383>
- 914 Singh, A. P., & Bhakar, P. (2021). Development of groundwater sustainability index: A case study
915 of western arid region of Rajasthan, India. *Environment Development and Sustainability*, 23,
916 1844-1868. <https://doi.org/10.1007/s10668-020-00654-9>
- 917 Songliao River Water Resources Commission of Ministry of Water Resources (SRWRC) (2017).
918 *Water allocation scheme of Tao'er River Basin*.
- 919 Sophocleous, M. (1997). Managing water resources systems: Why "safe yield" is not sustainable.
920 *Groundwater*, 35(4), 561. <https://doi.org/10.1111/j.1745-6584.1997.tb00116.x>
- 921 Tian, Y., Zheng, Y., Wu, B., Wu, X., Liu, J., & Zheng, C. (2015). Modeling surface water-
922 groundwater interaction in arid and semi-arid regions with intensive agriculture.
923 *Environmental Modelling & Software*, 63, 170-184.
924 <https://doi.org/10.1016/j.envsoft.2014.10.011>

- 925 Tian, Y., Zheng, Y., Zheng, C., Xiao, H., Fan, W., Zou, S., et al. (2015). Exploring scale-dependent
926 ecohydrological responses in a large endorheic river basin through integrated surface water-
927 groundwater modeling. *Water Resources Research*, 51(6), 4065-4085.
928 <https://doi.org/10.1002/2015WR016881>
- 929 Thomas, B. F. (2019). Sustainability indices to evaluate groundwater adaptive management: a case
930 study in California (USA) for the Sustainable Groundwater Management Act. *Hydrogeology*
931 *Journal*, 27(1), 239-248. <https://doi.org/10.1007/s10040-018-1863-6>
- 932 Thomas, B. F., Caineta, J., & Nanteza, J. (2017). Global assessment of groundwater sustainability
933 based on storage anomalies. *Geophysical Research Letters*, 44, 11445–11455.
934 <https://doi.org/10.1002/2017GL076005>
- 935 Thomas, B. F., Famiglietti, J. S., Landerer, F. W., Wiese, D. N., Molotch, N. P., & Argus, D. F.
936 (2017). GRACE Groundwater Drought Index: Evaluation of California Central Valley
937 groundwater drought. *Remote Sensing of Environment*, 198, 384-392.
938 <https://doi.org/10.1016/j.rse.2017.06.026>
- 939 Tomaszewicz, M., Abou Najm, M., & El-Fadel, M. (2014). Development of a groundwater
940 quality index for seawater intrusion in coastal aquifers. *Environmental Modelling and*
941 *Software*, 57, 13-26. <https://doi.org/10.1016/j.envsoft.2014.03.010>
- 942 Useviciute, L. & Baltreinaite-Gedienė, E. (2022). Modelling of a Capillary Rise Height of Biochar
943 by Modified Lucas-Washburn Equation. *Environmental Modeling and Assessment*, 27(1), 29-
944 43. <https://doi.org/10.1007/s10666-021-09782-6>
- 945 Wang, D., Zhao, C., Zheng, J., Zhu, J., Gui, Z., & Yu, Z. (2021). Evolution of soil salinity and the
946 critical ratio of drainage to irrigation (CRDI) in the Weigan Oasis in the Tarim Basin. *Catena*,
947 201, 105210. <https://doi.org/10.1016/j.catena.2021.105210>
- 948 Wang, M., Xu, B., Li, Y., Han, F., Du, X., Zhang, J., et al. (2023). A surface and ground-water
949 integrated investigation of streamflow drying up in semi-arid regions. *Hydrological*
950 *Processes*, 37(6), e14903. <https://doi.org/10.1002/hyp.14903>
- 951 Wang, W., Li, J., Wang, W., Chen, X., Cheng, D., & Jia, J. (2014). Estimating streambed
952 parameters for a disconnected river. *Hydrological Processes*, 28(10), 3627-3641.
953 <https://doi.org/10.1002/hyp.9904>

- 954 Water Resources Management Center of Baicheng City (WRMC) & Water Conservancy Survey
955 and Design Institute of Baicheng City (WCSDI). (2015). *Water resources comprehensive*
956 *planning report of Baicheng City*.
- 957 Wilcke, R. A. I., Mendlik, T., & Gobiet, A. (2013). Multi-variable error correction of regional
958 climate models. *Climatic Change*, 120(4), 871-887. [https://doi.org/10.1007/s10584-013-](https://doi.org/10.1007/s10584-013-0845-x)
959 [0845-x](https://doi.org/10.1007/s10584-013-0845-x)
- 960 Xu, W., & Su, X. (2019). Challenges and impacts of climate change and human activities on
961 groundwater-dependent ecosystems in arid areas - A case study of the Nalenggele alluvial fan
962 in NW China. *Journal of Hydrology*. 573, 376-385.
963 <https://doi.org/10.1016/j.jhydrol.2019.03.082>
- 964 Yan, D., Weng, B., Wang, G., Wang, H., Yin, J., & Bao, S. (2014). Theoretical framework of
965 generalized watershed drought risk evaluation and adaptive strategy based on water resources
966 system. *Natural Hazards*, 73(2), 259-276. <https://doi.org/10.1007/s11069-014-1108-5>
- 967 Yang, Z., Li, W., Li, X., & He, J. (2019). Quantitative analysis of the relationship between
968 vegetation and groundwater buried depth: A case study of a coal mine district in Western
969 China. *Ecological Indicators*, 102, 770-782. <https://doi.org/10.1016/j.ecolind.2019.03.027>
- 970 Ye, S., Xue, Y., Wu, J., Yan, X., & Yu, J. (2016). Progression and mitigation of land subsidence in
971 China. *Hydrogeology Journal*, 24(3), 685-693. <https://doi.org/10.1007/s10040-015-1356-9>
- 972 Yoneda, M., Morisawa, S., Takine, N., Fukuhara, S., Takeuchi, H., Hirano, T., et al. (2001).
973 Groundwater deterioration caused by induced recharge: Field survey and verification of the
974 deterioration mechanism by stochastic numerical simulation. *Water Air and Soil Pollution*,
975 127(1-4), 125-156. <https://doi.org/10.1023/A:1005251716246>
- 976 Yu, Z. (2003). *Monographs on Crop Cultivation (Northern Version)*. Beijing: China Agriculture
977 Press.
- 978 Zhai, J., Dong, Y., Qi, S., Zhao, Y., Liu, K., & Zhu, Y. (2021). Advances in Ecological
979 Groundwater Level Threshold in Arid Oasis Regions. *Journal of China Hydrology*, 41(1), 7-
980 14. <https://doi.org/10.19797/j.cnki.1000-0852.20195391>
- 981 Zhang, C., Shao, J., Li, C., & Cui, Y. (2003). A study on the ecological groundwater table in the
982 North China Plain. *Journal of Jilin University (Earth Science Edition)*, (03), 323-326+330.

<https://doi.org/10.13278/j.cnki.jjuese.2003.03.013>

Zhang, C., Xu, B., Li, Y., & Fu, G. (2017). Exploring the Relationships among Reliability, Resilience, and Vulnerability of Water Supply Using Many-Objective Analysis. *Journal of Water Resources Planning and Management*, 143(8), 04017044. [https://doi.org/10.1061/\(ASCE\)WR.1943-5452.0000787](https://doi.org/10.1061/(ASCE)WR.1943-5452.0000787)

Zhang, H., Singh, V. P., Sun, D., Yu, Q., & Cao W. (2017). Has water-saving irrigation recovered groundwater in the Hebei Province plains of China? *International Journal of Water Resources Development*, 33(4), 534-552. <https://doi.org/10.1080/07900627.2016.1192994>

Zhang, R., Wu, J., Yang, Y., Peng, X., Li, C., & Zhao, Q. (2022). A method to determine optimum ecological groundwater table depth in semi-arid areas. *Ecological Indicators*, 139, 108915. <https://doi.org/10.1016/j.ecolind.2022.108915>

Zhang, T. (1981). Water resources utilization and ecological environment in arid regions of China. *Natural Resources*, (01), 62-70.

Zhang, Y., Yu, J., Qiao, M., & Yang, H. (2011). Effects of eco-water transfer on changes of vegetation in the lower Heihe River basin. *Journal of Hydraulic Engineering*, 42(07), 757-765. <https://doi.org/10.13476/j.cnki.nsbdkk.2017.01.015>

Zhao, H. (2012). Study on ecological groundwater level and the amount of regulation in plain region of western Jilin Province, (Doctoral dissertation). Retrieved from China National Knowledge Internet. (<http://cdmd.cnki.com.cn/article/cdmd-11415-1012364424.htm>). Beijing: China University of Geosciences (Beijing).

Zhao, Q., Zhang, B., Yao, Y., Wu, W., Meng, G., & Chen, Q. (2019). Geodetic and hydrological measurements reveal the recent acceleration of groundwater depletion in North China Plain. *Journal of Hydrology*, 575, 1065-1072. <https://doi.org/10.1016/j.jhydrol.2019.06.016>